# GRACE D-103133

Gravity Recovery and Climate Experiment
Follow-on (GRACE-FO)

Level-3 Data Product
User Handbook

May 10, 2021

Jet Propulsion Laboratory
California Institute of Technology

Prepared by:

        Felix W. Landerer,
        NASA Jet Propulsion Laboratory, California Institute of Technology

        Savannah S. Cooley,
        NASA Jet Propulsion Laboratory, California Institute of Technology

        Contact Information:
            NASA Jet Propulsion Laboratory
            4800 Oak Grove Dr.,
            Pasadena, CA 91109, USA
            Email: grace-fo@jpl.nasa.gov

Reviewers:
        Vincent Humphrey,
        California Institute of Technology

        John T. Reager,
        NASA Jet Propulsion Laboratory, California Institute of Technology

        Margaret M. Srinivasan,
        NASA Jet Propulsion Laboratory, California Institute of Technology

Document Change Record

Issue	Date	Pages	Change Description
1.0	2018-10-08	All	First Version 1.0 - DRAFT
1.1	2019-01-19	25-57	Comments from Felix Landerer incorporated.
1.2	2019-03-27	All	Comments from Vincent Humphrey incorporated.
1.3	2020-07-07		Updated GRD-3 file naming convention
1.4	2021-05-10		V4 Tellus Data Update & description ([1] incorporating ellipsoidal correction for Level-3 grids; [2] monthly uncertainty estimates)

TABLE OF CONTENTS

1. INTRODUCTION

The Gravity Recovery and Climate Experiment Follow-on (GRACE-FO) mission succeeds the GRACE mission, which launched on March 17, 2002. In more than 15 years of operation, GRACE provided pioneering observations of global mass flux that significantly contributed to our understanding of large-scale changes in polar ice, soil moisture, surface and ground water storage, and ocean mass distribution. GRACE-FO launched on May 21, 2018, and its primary mission goal is to continue the tracking of Earth's mass movements and changes, in particular those related to water. The GRACE-FO mission is a partnership between NASA and the German Research Centre for Geosciences (GFZ).

This GRACE-FO Level-3 Data Handbook is designed to guide both experienced and beginner users in understanding and using Level-3 GRACE and GRACE-FO data products. The three main objectives of this document are to, 1) provide an overview of the GRACE-FO mission including the instrument design, science data processing, and calibration and validation procedures, 2) provide a description of the available Level-3 GRACE-FO data products and featured science and applications of Level-3 GRACE and GRACE-FO data, and 3) provide a set of step by step, reproducible use cases intended to serve as a reference for users who are interested in GRACE-FO Level-3 data products.

2. INSTRUMENT DESIGN

The instruments on GRACE and GRACE-FO were designed to enable measurements of the mean and time-variable components of the Earth's gravity field variations. They can detect gravitational differences on the planet's surface equivalent to that of a 300-km disk of water only one centimeter thick. GRACE-FO uses the same method to measure gravitational fields as the GRACE mission. Unique to the GRACE missions, the two satellites *are* the measurement instrument. GRACE-FO's two satellites follow each other in orbit around the Earth, separated by about 137 miles (220 km). Small changes in the distance between the two satellites, which result from the variable pull of gravity on each as they pass over the Earth's surface, make up the measurement. Both satellites are capable of flying either in the lead or trailing positions, forward or backward into the residual atmospheric wind. The mass of each GRACE-FO satellite is approximately 600 kg, including about 30 kg of nitrogen fuel propellant used for orbit control maneuvers.

A microwave ranging system measures the variations of the separation distance of the satellites to within one micron, about the diameter of a blood cell. The instrument is a K-Band Ranging System and it precisely measures the changes in the separation between the two GRACE satellites using phase tracking of K- and Ka-band microwave signals sent between the two satellites in a configuration known as DOWR (Dual One Way Ranging). Each satellite transmits carrier phase to the other at two frequencies, allowing for ionospheric corrections. K-band has a radio frequency of about 24 GHz and Ka-band is near 32 GHz. The range variations can be reconstructed from these phase measurements and its numerically derived derivatives, along with

other mission and ancillary data, is subsequently analyzed to compute the parameters of an Earth gravity field model that reflects the planetary mass distribution for a particular month.

Spatial and temporal variations in the Earth's gravity field affect the twin spacecraft differently, causing changes in the distance between the spacecraft as they orbit the Earth. For instance, when the GRACE-FO satellite pair pass over an area of the Earth with a positive gravitational anomaly, the change in gravitational field affects the lead satellite first, pulling it away from the trailing satellite. As the satellites continue, the trailing satellite is pulled toward the lead satellite as it passes over the gravity anomaly.

The microwave ranging instrument used by GRACE and GRACE-FO is referenced to a ultrastable quartz clock and coupled with precise Satellite Global Positioning System (GPS) receivers, which determine the position of the satellite over the Earth to within a centimeter or less.

A highly accurate electrostatic, temperature-controlled accelerometer, which is located at each satellite's center of mass, measures the non-gravitational accelerations of the satellites, which include air drag, solar radiation pressure, and attitude control activator operation. Measuring the non-gravitational forces on each satellite in this way serves to ensure that only accelerations caused by gravity are considered in the distance measurements. The Star Camera Assembly is comprised of star cameras (three on GRACE-FO, two on GRACE) mounted close to the accelerometer on each satellite to provide the precise attitude references for the satellites.

In addition to the microwave ranging system (which is based on the corollary instrument on GRACE), GRACE-FO also has an experimental laser ranging instrument, which is designed to make the measurement of the separation distance between the two spacecraft (the primary measurement) even more precise. This advanced laser instrument could improve the accuracy of inter-spacecraft ranging by tenfold or more and lead to significantly enhanced gravity measurements and future missions.

3. GRACE-FO SCIENCE DATA PROCESSING SYSTEM

Since GRACE's launch in March 2002, the official GRACE Science Data System (SDS) continuously releases monthly gravity solutions from three different processing centers. GRACE-FO data will also be distributed in these processing centers (links to each can be found in Section 7.1):

- Jet Propulsion Laboratory (JPL)

- Center for Space Research at University of Texas, Austin (CSR)

- GeoforschungsZentrum Potsdam (GFZ)

Deriving month-to-month gravity field variations from GRACE and GRACE-FO observations requires a complex inversion of relative ranging observations between the two spacecraft, in combination with precise orbit determination via GPS and various corrections for spacecraft accelerations not related to gravity changes (Figure 1). GRACE and GRACE-FO data appear in three different processing centers because many parameter choices and solution strategies that are possible. GFZ, CSR, and JPL explore these solution strategies differently. The differences in the resulting Level-2 gravity fields have helped to better understand the characteristics of the various approaches, and differences between the centers' processing strategies have generally decreased over the Releases.

The varied solutions from JPL, CSR, and GFZ can be used to infer the uncertainty in Level-2 and Level-3 GRACE and GRACE-FO fields that arises from the choice of solution strategy. Recent papers (e.g., Sakumura et al., 2014) found that the ensemble mean (simple arithmetic mean of JPL, CSR, GFZ fields) was effective in reducing the noise in the gravity field solutions within the available scatter of the solutions. We recommend that users average all three data center's solutions (JPL, CSR, GFZ).
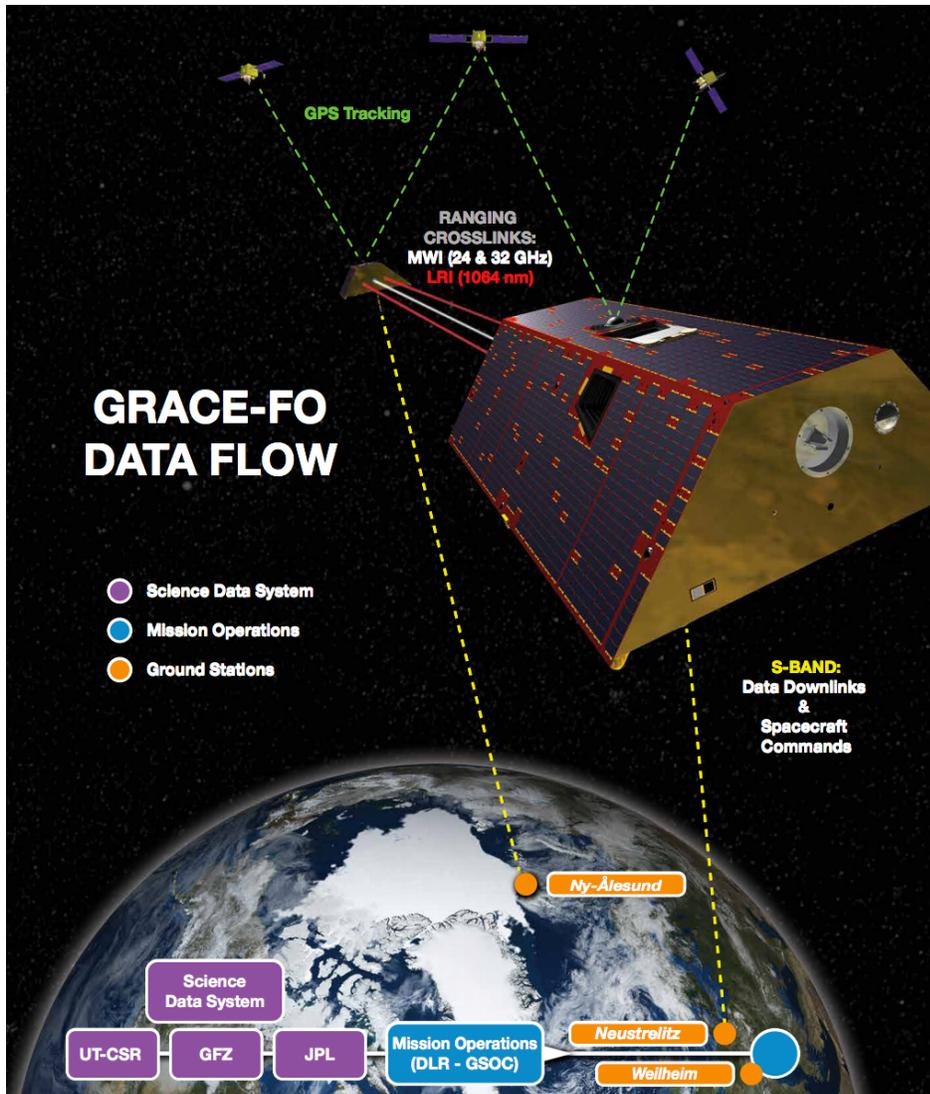
Figure 1 This graphic shows the GRACE and GRACE-FO Mission Science Data System and Flow. Data travel from the GRACE and GRACE-FO satellites to receivers on the ground. The measurement and housekeeping data are stored onboard the GRACE-FO satellites and relayed to ground stations when the satellites pass over at least once a day.

3.1 Level-1 Processing

Collectively, the processing from Level-0 to Level-1B is called the Level-1 Processing. Please refer to the GRACE and GRACE-FO Level-1B Data Product User Handbooks for more information on Level-1 processing.

3.2 Level-2 Processing

GRACE and GRACE-FO Level-2 gravity field data products contain a set of spherical harmonic coefficients of the "geopotential". "Geopotential" refers to the exterior potential gravity field of the Earth system, which includes its entire solid and fluid (including oceans and atmosphere) components. The geopotential at a fixed location is variable in time due to mass movement and exchange between the Earth system components. The continuum of variations of the geopotential

is represented by theoretically continuous variation of the geopotential coefficients. Following conventional methods (Heiskanen & Moritz 1967), at a field point that is exterior to the Earth system, the potential of gravitational attraction between a unit mass and the Earth system may be represented using an infinite spherical harmonic series. Though the exact spherical harmonic expansion of the geopotential requires an infinite series of harmonics, the expansion is effectively limited to a maximum degree (approx. 60-100 for GRACE and GRACE-FO monthly fields, and >150 for long-term mean fields). Degree 60 corresponds to spatial length scales of about 330 km.

Three centers are part of the GRACE Ground System and generate the spherical harmonic fields for the Level-2 data product: CSR, GFZ and JPL. Their output includes spherical harmonic coefficients of the gravity field, as well as the dealiasing fields used in the data processing. For a detailed description of the Earth gravity field estimates provided by the Level-2 processing and the background gravity models used, please refer to the Level-2 Gravity Field Product User Handbooks for each center.

3.3 Level-3 Processing

3.3.1 Overview

Observed monthly changes in gravity are caused by monthly changes in mass. Most of the monthly gravity changes are caused by changes in water storage in hydrologic reservoirs, by moving ocean, atmospheric and land ice masses, and by mass exchanges between these Earth system compartments. As such, gravity measurements from space provide a precise measure of mass redistribution of Earth's water cycle. Their vertical extent is measured in equivalent water height (also known as equivalent water thickness).

The transformation of the gravity potential into Earth surface mass changes requires the application of various steps to account for a number of different processes including the removal of correlated and random errors, glacial isostatic adjustment (GIA), as well as other background model corrections.

The land and ocean grids (also known as mass concentration blocks or simply, "mascons") are typically processed with domain-optimized filters that are tuned to best filter out noise while preserving real geophysical signals. The key processing steps from Level-2 spherical harmonic data to Level-3 gridded mascon solutions are summarized in **Error! Reference source not found.**2.
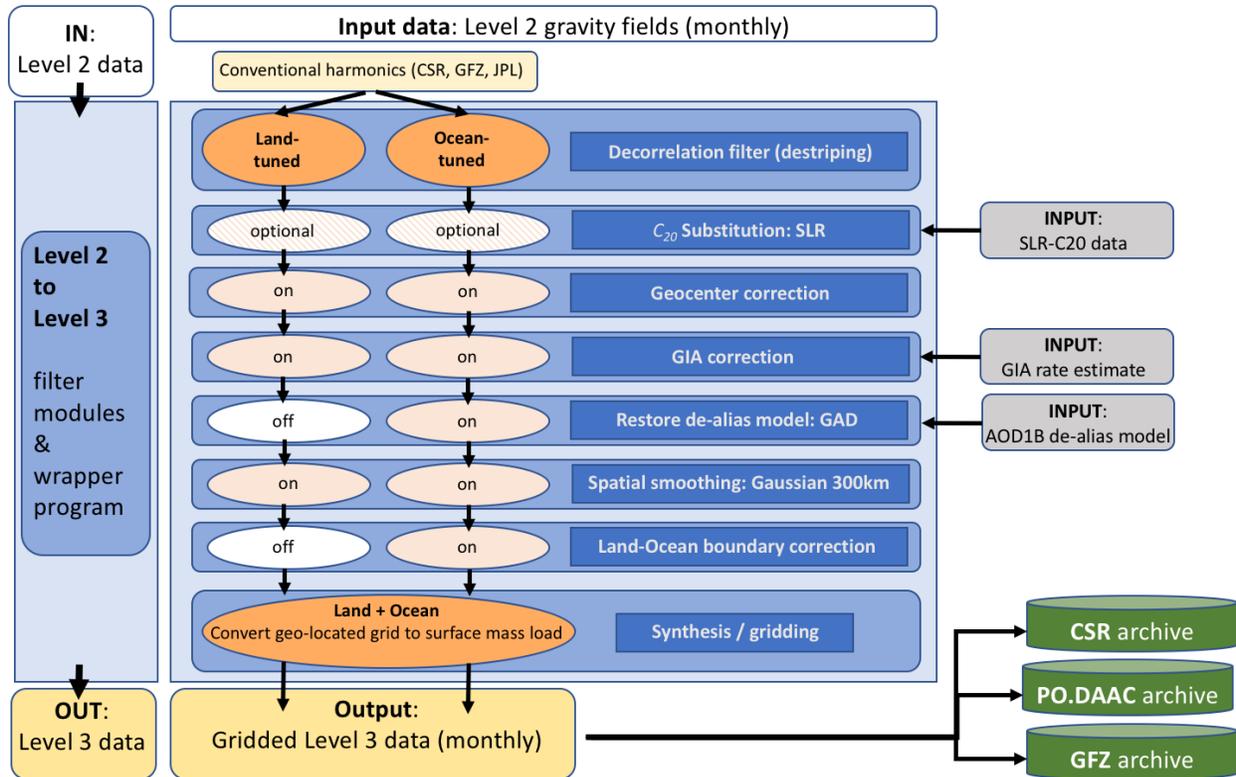
Figure 2 Flowchart and overview of GRACE and GRACE-FO Level-3 sequential processing steps for conventional Level-2 spherical harmonic solutions. The land and ocean grids are processed with different filters that are tuned to best filter out noise while preserving real geophysical signals.

3.3.2 Decorrelation filter (de-striping)

Unconstrained monthly GRACE and GRACE-FO Level-2 solutions contain errors that arise from both random measurement errors as well as from correlated noise. The presence of correlated error in GRACE and GRACE-FO data manifests itself mostly as North-South stripes due to a lack in observability in the plane orthogonal to the satellites' orbit. Several filters, most of which are empirical, exist to remove this correlated error (e.g., Duan et al., 2009; Chambers and Bonin, 2012). The filter used in Level-3 GRACE and GRACE-FO data processing to remove correlated error uses a destriping technique, based on approach described by Swenson and Wahr (2006), but adapted to more recent data releases.

3.3.3 Spherical Harmonic Coefficient C2,0 Substitution

In contrast to degree-one coefficients, higher-order degrees (degree≥2) are directly observed by GRACE and GRACE-FO. However, it has been noted that some long-wavelength, low-degree geoid field coefficients from GRACE and GRACE-FO can be noisy. In particular, the spherical harmonic coefficient C_{20} (degree 2 and order 0) from GRACE and GRACE-FO Level-2 monthly solutions contains errors. Satellite-Laser-Ranging (SLR), on the other hand, currently provides more accurate measurements of the monthly variations of the C_{20} coefficient (Cheng et al., 2013). Therefore, C_{20} coefficients are replaced with the solutions from SLR (Cheng et al., 2011), which are processed with GRACE and GRACE-FO compatible background models.

For more information on C_{20} substitution with SLR and J2, see the technical note TN-11_C20_SLR, which contains the Level-2 gravity field-compatible C_{20} coefficients and links to relevant documentation (ftp://podaac.jpl.nasa.gov/allData/grace/docs/).

3.3.4 Geocenter correction

The GRACE and GRACE-FO satellites measure gravity changes in the Earth's center of mass (CM) reference frame. By definition, the combined solid Earth and all surface mass changes yield spherical harmonic degree-one (referred to as geocenter) Stokes coefficients equal to zero relative to the center of mass, and GRACE and GRACE-FO measurements alone cannot recover the degree-one coefficients directly. However, the omission of spherical harmonic degree-one coefficients can introduce significant biases in particular for seasonal surface mass variations as well as bias trends that arise when evaluating mass transport in the center of figure (i.e., relative to the solid Earth).

Because of their physical meaning, time changes in degree 1 coefficients can be expressed in several equivalent forms:

1. As distances in mm between the center of mass and the center of figure along the Z (axis of rotation), X and Y axes;
2. As fully normalized coefficients of the geopotential;
3. As the changes in mass (per unit area) that would give rise to the geopotential coefficients, expressed either in kg/m^2 or equivalent water height.

GRACE and GRACE-FO cannot retrieve spherical harmonic coefficients of degree 1 proportional to the position of the Earth's geocenter relative to an Earth-fixed reference frame. GRACE and GRACE-FO Level-3 processing uses an estimate of these coefficients based on Swenson et al. (2008), a method that uses both higher order gravity estimates and the forward-modeled geocenter contributions assuming the ocean contribution is known (e,g., from a model). GRACE and GRACE-FO geocenter coefficients computed in this manner are available at ftp://podaac.jpl.nasa.gov/allData/tellus/L2/degree_1/. These coefficients are expressed in the form (2) above.

3.3.5 Glacial Isostatic Adjustment

Some changes in gravity are caused by mass redistribution in the 'solid' Earth, including those due to glacial isostatic adjustment (GIA) of the lithosphere and mantle, which occur due to lithospheric viscous adjustment from the glacial loading of the last ice age. In those cases, the interpretation of the gravity changes in terms of equivalent water thickness are not correct. The standard Level-3 GRACE-Tellus mass grids have had a GIA model of secular trends removed, in terms of (apparent) mass change. Note that different GIA models exist and are frequently updated.

3.3.6 Land and Ocean De-aliasing Models

High frequency variations in the Earth's gravity field caused by both the atmosphere and the ocean at sub-monthly (hourly to few days and weeks) periods would alias into the monthly

gravity data due to insufficient sampling, and thus need to be corrected. The process of removing these high frequency variations with models is known as "de-aliasing."

The mass of the atmosphere is removed during Level-2 processing using atmospheric pressure fields from the Integrated Forecasting System (IFS / ECMWF). As a result, the GRACE Tellus surface mass grids do not contain atmospheric mass variability over land or continental ice areas like Greenland and Antarctica except for errors in ECMWF.

To avoid spatial and temporal aliasing of sub-monthly ocean mass changes (including tides), ocean mass changes are also forward-modeled and removed during the Level-2 GRACE processing. The ocean model removes high frequency (six-hourly to sub-monthly) wind and pressure-driven ocean motions that might otherwise alias into the monthly gravity solutions. The resulting monthly GRACE/GRACE-FO gravity fields effectively represent corrections to the ocean model. To use the data over the oceans, the GRACE Tellus ocean bottom pressure fields include the monthly averaged ocean model grids added back to the gravity coefficients (for more information, see Chambers and Bonin, 2012).

Details on the dealiasing GRACE and GRACE-FO AOD1B products as well as on the precursor releases can be found in the GRACE AOD1B Product Description Document (Fletchner et al., 2015).

3.3.7 Spatial smoothing
While a significant amount of correlated errors can be removed with the de-correlation filter, an additional filter step is often employed to reduce remaining noise. This reduction can be achieved by applying a spatial smoothing filter. A simple isotropic Gaussian filter can be formulated in the spherical harmonic domain as (e.g., Chambers 2006). The smoothing radius is 300 km for land grids, and 500km for ocean grids.

3.3.8 Spatial Leakage Correction
Due to the limited spatial resolution of GRACE and GRACE-FO, the signal separation along land-ocean boundaries is also limited. Large signals that actually occur over land can 'leak' into the adjacent ocean areas and give the false appearance of large ocean bottom pressure changes while in reality these signals actually occur over land (e.g., Chambers and Bonin, 2012). An iterative solution to compute the 'leaked' signals and improve the land-ocean signal separation was first proposed by Wahr et al., (1998), and has since been improved and fine-tuned by Chambers and Bonin (2012). The leakage correction is applied only to the ocean grids. In principle it goes both ways (i.e., ocean signals 'leaking' onto land), but since ocean signals are typically significantly smaller than land signals, the ocean-to-land leakage is (mostly) negligible.

3.3.9 Spatial Synthesis & Gridding
The last step in the Level-2 to Level-3 processing involves the mapping of the data from the spherical harmonic domain into a geo-referenced grid, typically a global regular grid of 1 or 0.5 degree latitude / longitude resolution. (Wahr et al., 1998). As of Tellus Version 4 (V4) of the Level-3 land (LND) and ocean (OCN) grids, an additional ellipsoidal correction has been applied to the standard spherical harmonic gravity coefficeints to account for the fact that the Earth's

shape deviates significantly from a sphere, and is better approximated by an ellipsoid (e.g, Ghobadi-Far et al., 2019). The effect of the ellipsoidal correction is largest in polar regions, and tends to result in larger signals (e.g, annual amplitudes and trends) in those regions compared to a simple spherical harmonic synthesis (Figure 3).
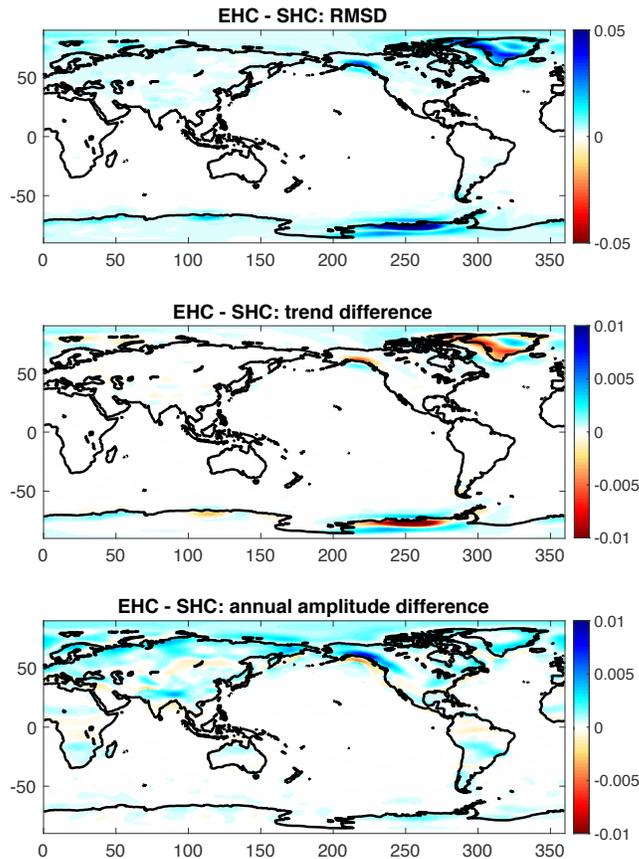

Figure 3 Differences of JPL RL06 surface mass changes with the ellipsoidal correction (Ghobadi-Far et al., 2019) applied, relative to the standard spherical harmonic synthesis. top: RMS difference; middle: trend difference; bottom: annual amplitude difference. Units: [meters-H2O]. Time period covered: 02/2004 – 03/2021.

4. SCIENCE DATA CALIBRATION AND VALIDATION

Unlike most NASA Earth Observing missions, it is not possible for GRACE and GRACE-FO science measurements to be directly calibrated to ground measurements. For example, missions that measure specific regions in the electromagnetic spectrum use a radiometer for calibration, there is no equivalent instrument to calibrate the gravity-related range rate measurements.

However, there are a few methods to validate GRACE and GRACE-FO Level-3 data products. The first approach involves comparing the data against independent proxy data. The second approach uses a "null test" or "quiet region" to estimate noise floors. The third approach harnesses a priori information from known mass variations, which can be obtained with radar altimetry measures of large water bodies such as lakes or reservoirs (Table 1).

Validation	
Over land / inland lakes	lake level; 'quiet' desert regions to identify noise floor
Over oceans	bottom pressure recorders (BPR); 'quiet' ocean regions to identify noise floor

Table 1 The main techniques or quantities that can be used to validate GRACE and GRACE-FO observations. The approaches to validate GRACE data can be broken into categories based on whether the data product covers land, ocean or land-ice.

4.1 Validation with ocean bottom pressure recorders

Ocean bottom pressure recorders (BPRs) can be used as a proxy for direct comparison with Level-3 GRACE and GRACE-FO data. BPRs measure the mass of the overlying water column plus that of the atmosphere. Validation with independent BPR measurements give some indication of the quality of the available GRACE estimates, although the sparseness of the available BPR sites limits the generality of conclusions. The BPR data variance can be associated with short-scale, localized effects, which may not be fully resolved in relatively coarse resolution estimates provided by GRACE and GRACE-FO. An effective way to overcome the issues caused by the difference in spatial resolutions between BPRs and GRACE is to average out the effects of eddies from multiple BPRs when such array data is available.

For instance, Morrison et al. (2007) compare Arctic BPR measurements from two instruments in about 4,250 m depth with GRACE. The study shows differences of 3.10 cm RMS mainly at 1–2 month time scales, with higher agreement at monthly to sub-annual time-scales. Some of the difference is likely due to comparing the Arctic BPR measurements point measurements with the inherent spatial averages of the satellite observations. This issue can be addressed by averaging the BPR measurements across locations.

Another challenge in using BPRs to validate GRACE and GRACE-FO solutions arises because of the relatively small signal of bottom pressure variations. Peralta-Ferriz et al. (2014) find that even with optimizing GRACE solutions to reduce leakage from major glacial melt regions of their study area (Greenland, Iceland, and Svalbard), the amplitude of the hydrologic signals from

the terrestrial Arctic watersheds (Ob, Yenisey, Pechora, etc.) are larger than the ocean gravity change, and thus may leak into the oceanic signals measured by GRACE and GRACE-FO.

4.2 Validation with the null test

The second approach for validating GRACE and GRACE-FO data involves using a "null test" in which GRACE and GRACE-FO time series are examined over regions of known small or zero water movement. Any detected mass movement in these regions can be attributed to noise. Because of its large scale, the Sahara desert is one of the best possible candidates to conduct a null test experiment. Boy et al. (2012) conduct a null test validation experiment over the Sahara and Libya deserts. They estimate that the errors of GRACE continental water storage are about 10 to 20 mm over their study area. On the other hand, even in very dry regions like these there may be long-term changes due to aquifer and groundwater changes that are real signals, and therefore care should be taken to assume a 'zero-signal' region.

4.3 Validation with known mass variations

A third way to validate GRACE and GRACE-FO solutions is to compare mass estimates with known mass variations. As a result of several decades of radar altimetry, water Level-variations of major lakes and reservoirs are monitored with a precision of a few centimeters. These induced volume variations should be equivalent to the mass variations as retrieved by GRACE and GRACE-FO, if thermal expansion is neglected (or otherwise accounted for).

Longuevergne et al. (2013) use a priori information on reservoir storage from radar altimetry and conduct an analysis testing effects of location and areal extent of reservoirs within a basin on basin-wide average water storage changes, with application to the lower Nile (Lake Nasser) and Tigris-Euphrates basins as examples. Findings suggest that the impact of the concentrated mass on water storage changes depends on the location and areal extent of the reservoirs, the basin area, and GRACE processing. Forward modeling shows that if reservoir storage is assumed to be uniformly distributed, then the result may be an underestimation (when near the basin center) or overestimation (near the basin margin) by up to a factor of 2, depending on reservoir location and areal extent. In addition, mass changes outside a basin of interest may contribute significantly because of leakage into the basin.

As findings from Longuevergne et al. (2013) and others suggest, GRACE and GRACE-FO estimates in regions with lakes and reservoirs require careful interpretation because of the significant storage volumes, small spatial footprint (often unresolved by GRACE and GRACE-FO) and relatively short time response (compared to groundwater), especially when attempting to separate changes in GWS in agricultural regions where both surface and groundwater are used conjunctively.

5. LEVEL-3 DATA PRODUCTS

5.1 Known Uncertainties & Sources of Error

5.1.1. Level-2 Data Processing Errors

All Level-3 GRACE and GRACE-FO data have errors and uncertainties inherited from the satellite-level measurements and Level-2 processing. The background gravity model used for Level-2 data processing contains errors of omission, as well as errors of commission.

The collection of background models is used in GRACE and GRACE-FO Level-2 data processing to make a prediction of the observable range change or its derivatives. The difference between the observed and predicted values of the measurements is the residual, which exists because of the errors of omission and commission, in addition to the measurement errors and model deficiencies or incompleteness. The background gravity model errors may be expected to have continual spatial-temporal variability. An update to the background gravity model is computed such that the measurement residuals are minimized in the least-squares sense – and this update may be regarded as the new gravity information available from GRACE and GRCE-FO. In the science data processing, at the most elementary level, this update to the geopotential is parametrized, for a selected data span, as a set of constant corrections to the spherical harmonic coefficients of the geopotential, to a specified maximum degree and order.

5.1.2 Correlated Error, Spatial Smoothing and Leakage Error

The uncertainty of gridded Level-3 surface mass change products is a function of both measurement errors as well as signal leakage errors (Landerer and Swenson, 2012). Measurement errors include systematic and random errors, which are reduced by applying the de-correlation and Gaussian smoothing filters, respectively.

While destriping and smoothing filters are typically successful in removing the correlated error, they have also been shown to remove real geophysical signals from the data which mimic the North-South striping pattern of the error. To compensate for this, a global set of gain factors (limited to continental hydrology applications) has been developed (Landerer and Swenson, 2012) to restore signal amplitudes which were removed in the filtering process. However, these gain factors can potentially introduce biases in frequency bands outside the annual component, in particular for longer term trends. In those cases, kernel-specific gain factors are necessary (Landerer and Swenson, 2012; Rodell et al., 2009).

5.1.3 Glacial Isostatic Adjustment

GIA is not actually an error in GRACE and GRACE-FO data; in fact, GIA is a signal of great scientific interest in itself, as GRACE observations have provided new and more accurate estimates of GIA models, and have led to refinements of ice-load histories. However, the GIA corrections add some uncertainty for estimated surface mass trends over the GRACE period; a canonical uncertainty range of up to 20 percent is often assumed for GIA models.

5.1.4 Earthquakes

Large earthquakes can cause sufficient displacements of the Earth's lithosphere to generate a change in Earth's gravity field that GRACE measures. Some examples include the earthquakes

off the West Coast of Northern Sumatra (Indonesia) on December 24, 2004; Northern Sumatra on March 25, 2005; Southern Sumatra on September 12, 2007; offshore Maule, Chile on February 27, 2010; and near the East Coast of Honshu, off Tohoku, Japan on March 11, 2011. All the earthquakes mentioned above had magnitudes of 8.5 or higher.

As with GIA, earthquake-related changes in gravity would bias the derived 'equivalent water thickness' if not properly accounted for. While a GIA model is used to 'correct' the GRACE and GRACE-FO data, signals from large earthquakes are currently not removed from the GRACE and GRACE-FO data. Users should therefore be wary of signals in the vicinity of large earthquakes. A user can remove the signal due to an earthquake following the approach of de Linage et al. (2009); see their equation 3.

5.1.5 Atmosphere and Ocean De-aliasing Models
The removal of atmospheric effects in GRACE-FO data takes advantage of the output of numerical weather modelling and forecasting analysis groups around the world, including the National Centers for Environmental Prediction (NCEP, United States) and the European Center for Medium Range Weather Forecasting (ECMW). These groups assimilate in situ observations, including barometers, and produce pressure maps every 6 hours. Analysis of the quality of these pressure fields by Velicogna and Wahr (1999) indicate that they are generally of sufficient quality to remove pressure effects at the level of less than 1 mbar (or even 0.5 mbar or less for 30 day averages) in most regions.

Errors in de-aliasing models related to model drifts and changes can introduce biases GRACE estimates of mass change within basins. For instance, Hardy et al., (2017) show that over Antarctica, errors in AOD1B Release 05 (RL05) spuriously mask acceleration in mass loss on the order of 4 Gt yr^{-2}. Over Greenland, atmospheric errors are a major noise source and introduce a spurious trend of up to 2 Gt yr^{-1}. The released AOD1B RL06 mitigates some of these errors using a higher spatial resolution, more accurate input models, and better control of model-change biases.

5.1.6 Ocean Bottom Pressure
The uncertainty of the GRACE and GRACE-FO-derived ocean bottom pressure (OBP) values can be estimated with a variety of methods. For OBP values derived from Release-04 (RL04) GRACE coefficients, uncertainty has been estimated to be between 2 and 3 cm root-mean-square (RMS) depending on the type of processing, based on comparison to steric-corrected altimetry (Chambers, 2006; Chambers and Willis, 2010), output from an ocean model (Ponte et al., 2007; Quinn and Ponte, 2010), or bottom pressure recorders (Morison et al., 2007; Park et al., 2008).

Chambers & Bonin (2012) conduct a validation of RL05 GRACE-derived OBP estimates and focus attention on the deep ocean because (1) OBP variations are longer wavelength and more resolvable by GRACE, and (2) quantifying accurate statistics for the deeper ocean areas avoids biases from higher errors near the coast.

To conduct the OBP validation, Chambers & Bonin (2012) use a general ocean circulation model that is a version of the MIT general circulation model (Marshall et al., 1997) and is run at JPL as part of the Estimating the Circulation and Climate of the Ocean (ECCO) consortium. The version

of JPL ECCO used in the study is a baroclinic model forced by winds, pressure, and heat and freshwater fluxes from the National Center for Environmental Prediction (NCEP) operational analyzes products and also assimilates satellite altimetry.

Chambers & Bonin (2012) subtracted JPL ECCO OBP maps (unsmoothed) from the destriped and 300 km smoothed GRACE OBP maps and computed the standard deviation of the residuals. Results indicate that the standard deviation of residuals is generally less than 2 cm throughout the ocean, and often less than 1.5 cm (a significant improvement from RL04 residuals, where the standard deviation is generally greater than 2 cm, and often more than 3 cm). The standard error for GRACE-derived OBP was about 1 cm equivalent water thickness (EWT) in the low- and midlatitudes, and between 1.5 and 2 cm in the polar and subpolar oceans (see below for monthly uncertainty estimates).

5.1.7 Terrestrial Water Storage

Estimates of terrestrial water storage (TWS) variations suffer from signal degradation due to measurement errors and noise, which are manifested as both random errors that increase as a function of spherical harmonic spectral degree (Wahr et al., 2006), and systematic errors that are correlated within a particular spectral order (Swenson and Wahr, 2006). Landerer & Swenson (2012) use simulations of terrestrial water storage variations from land-hydrology models to infer relationships between regional time series representing different spatial scales. These relationships, which are independent of the actual GRACE data, are used to extrapolate the GRACE TWS estimates from their effective spatial resolution (length scales of a few hundred kilometers) to finer spatial scales ($\sim$100 km). Three scaling relationships are examined: a single gain factor based on regionally averaged time series, spatially distributed (i.e., gridded) gain factors based on time series at each grid point, and gridded-gain factors estimated as a function of temporal frequency. While regional gain factors have typically been used in previously published studies, Landerer & Swenson (2012) find that comparable accuracies can be obtained from scaled time series based on gridded gain factors. In regions where different temporal modes of TWS variability have significantly different spatial scales, gain factors based on the first two methods may reduce the accuracy of the scaled time series. In these cases, gain factors estimated separately as a function of frequency may be necessary to achieve accurate results. The study provides gridded fields of leakage and GRACE measurement errors that allow users to estimate the associated regional TWS uncertainties. The resulting measurement errors typically show a latitudinal dependence, with highest values near the equator (standard deviation of up to 35 mm), and decreasing towards the poles (standard deviation of 15 mm; see below for monthly uncertainty estimates).

5.1.7 Gridded Uncertainty Estimates for Tellus LND & OCN Level-3 grids

As of Tellus Level-3 Version 4 (L3_v4) spatially and temporally varying uncertainty estimates are provided with each monthly LND or OCN field. The error calculation follows Swenson & Wahr (2006), representing the RMS of the residual after removing a fit (consisting of: const+trend+annual+semin-annual + K2 alias + S2 alias) from all spherical harmonic coefficients. To account for varying errors over time, in particular during months with reduced sampling coverage and/or higher instrument noise, the RMS map is scaled during each month such that the ocean-mean value for that month corresponds the RMS-mean of the fit-residuals over the ocean area. The fit residuals are derived after all postprocessing steps discussed above.

5.1.8 Mascon Uncertainty

Mascon uncertainty estimates for JPL's Mascon grids are provided on a 0.5 degree grid in latitude and longitude. Note that the uncertainties provided are uncertainties associated with each mascon estimate, represented on this (oversampled) grid. For 3-degree mascons, there are 4,551 independent estimates of uncertainty represented on this grid. This is not the uncertainty associated with a single 0.5 degree pixel, which would be much higher.

To derive the uncertainty estimates, the formal covariance matrix over the ocean is scaled to match the error seen when comparing the GRACE data to in-situ ocean bottom pressure data. Over quiet areas in the ocean, this amounts to approximately 1 cm of uncertainty per mascon.

Over land, the formal uncertainty is scaled by 2, and roughly matches uncertainty estimates derived using methods described in Wahr et al., (2006). The provided estimates of uncertainty are regarded to be conservative. Since we implement a Kalman filter in the solution process to link adjacent months together temporally, monthly solutions both at the very beginning and end of the time series have slightly larger uncertainties than monthly solutions in the middle of the time series. A more detailed description is found in Wiese et al. (2016).

5.3.9 Months with Lower Accuracy

Users need to be aware that the monthly grids have higher errors when the orbit is near exact repeat, which leads to degraded gravity field estimates. Such months include July to December 2004, and Jan & Feb 2015. Another source of larger errors is a gap of data (several hours to several days) in a few months.

Towards the end of the GRACE data record, several months contain accelerometer measurements from only a single satellite; for those months, special 'ACC transplant' solutions have been computed, which show degraded data quality with higher noise. These months are 11/2016, 12/2016, 01/2017, 03/2017, 04/2017, 06/2017.

5.3.10 Data Gaps in GRACE starting in 2011

Active battery management started in 2011 due to the aging batteries on the GRACE satellites. During certain orbit periods over several consecutive weeks, no ranging data were collected and hence no gravity fields could be computed. These gaps occur approximately every 5-6 months, and last for 4-5 weeks (Figure 3).
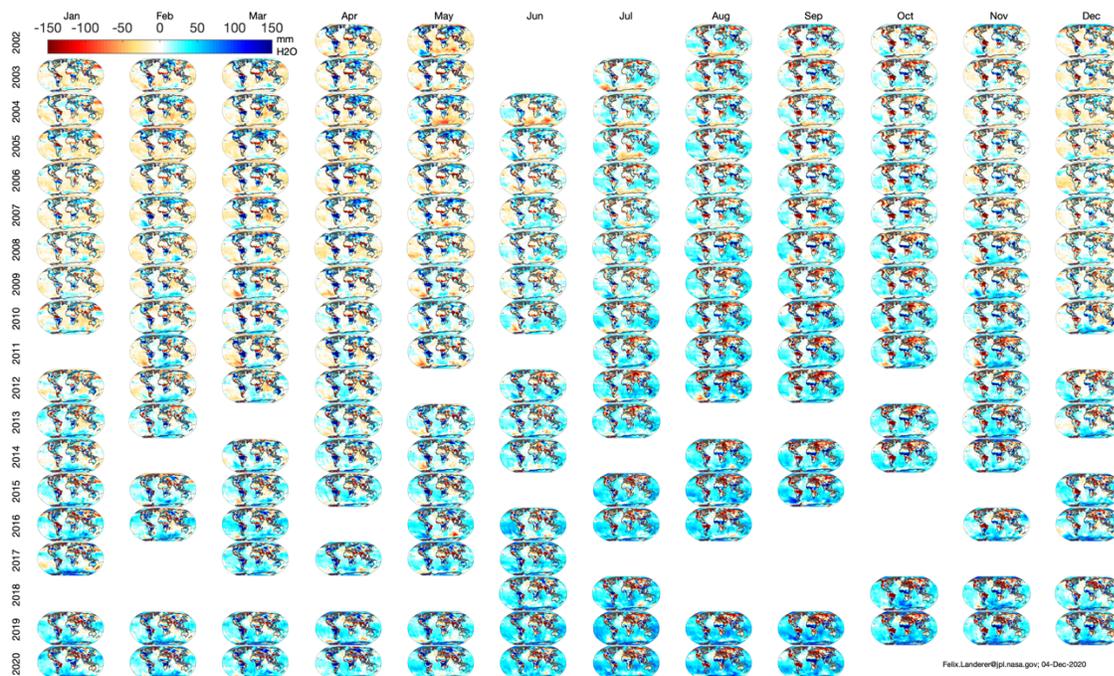
Figure 4 GRACE (2002-2017) and GRACE-FO (2018-06 onwards) data records, with gaps due to active battery management (started in 2011 due to the aging batteries on the GRACE satellites), and other instrument outages.

5.2 Mascon vs. Spherical Harmonics Comparison: Which Should I Use?
In general, users are encouraged to use the current gridded mascon data for several main reasons:

- Unlike the unconstrained spherical harmonic solutions, the constrained mascon solutions derived from geophysical models do not need to be destriped or smoothed and suffer less from leakage errors than harmonic solutions. For instance, Ocean bottom pressure (OBP) time series derived from the mascon solutions reduce the Root Mean Square error with respect to in situ data: Watkins et al. (2015) show a reduction of 0.37 cm globally, and as much as 1 cm regionally.

- The mascon approach allows a better separation of land and ocean signals with the coastline resolution improvement (CRI) filter coupled with the application of state of the art gain factors.

- Computing basin averages for hydrology applications shows general agreement between harmonic and mascon solutions for large basins; however, mascon solutions typically have greater resolution for smaller spatial regions, in particular when studying secular signals.

- The data processed from the spherical harmonic Level-2 data are not directly suited to accurately quantify ice mass changes over Greenland or Antarctica, or glaciers and ice caps. These regions require region-specific averaging kernels, as well as proper treatment of signal contamination from nearby land hydrology and adjusted GIA effects (see Jacob et al., 2012 for a thorough discussion of these aspects).

A caveat of the mascons is that it is not straightforward to quantify potential signal biases that could occur due to the addition of the a priori information. Watkins et al. (2015) note, however, that it is also difficult to quantify the exact amount of signal suppression that occurs when applying empirical post processing algorithms to remove correlated errors in the spherical harmonic gravity solutions. Derived gain factors are merely a good proxy for this and have considerable spatial variability.

Although improvements can be made in the details of the implementation of the mascon solutions, such as including deterministic geophysical processes (such as trends and annual signals) as state parameters and using smaller mascons to more accurately define coastlines and spatial constraints, the introduction of credible statistical geophysical information—either from models or from independent observations—to condition the gravity solution is ultimately preferable to relying on empirical ad hoc post processing techniques to remove correlated errors.

6. EXAMPLES OF GRACE AND GRACE-FO SCIENCE AND APPLICATIONS

6.1 2017 ESAS Decadal Survey Priorities

The National Research Council (NRC), led by the Space Studies Board in collaboration with other Earth Science related boards across the NRC, organized the 2017 Decadal Survey for Earth Science and Applications from Space (ESAS 2017), which aimed to generate consensus recommendations from the environmental monitoring and Earth science and applications community on an integrated and sustainable approach to the conduct of the U.S. government's civilian space-based Earth-system science programs. These programs are carried out predominantly by the National Aeronautics and Space Administration (NASA), the National Oceanic and Atmospheric Administration (NOAA), and the United State Geological Survey (USGS), with supporting and complementary contributions from agencies including the National Science Foundation (NSF), Department of Agriculture (USDA), Department of Energy (DoE), and Department of Defense (DoD).

ESAS 2017 presents a prioritized list of top-level science and application objectives to guide space-based Earth observations. From among hundreds suggested, ESAS 2017 addresses 35 key science and applications questions. Uses of GRACE and GRACE-FO data span all six categories that the 35 most important science and applications questions fall into:

- Coupling of the Water and Energy Cycles
- Ecosystem Change
- Extending & Improving Weather and Air Quality Forecasts
- Sea Level Rise
- Reducing Climate Uncertainty & Informing Societal Response
- Surface Dynamics, Geological Hazards and Disasters

Sections 6.2 through 6.10 illustrate key GRACE and GRACE-FO science and applications. Each of the featured advancements made in science and applications with GRACE and GRACE-FO data connects with one or more of the six priority categories the ESAS 2017 reports highlights.

6.2 Groundwater

A key application of GRACE-FO data is in groundwater monitoring. As climate change continues to exacerbate drought conditions, reliance on groundwater for agricultural and other uses increases globally. Therefore, obtaining data that can track changes in groundwater levels plays a critical role in informing societal response to climate uncertainty and water scarcity, in particular in regions where groundwater supplies the bulk of the water required for irrigation.

For instance, Rodell et al. (2009) assess long-term groundwater storage variation in the Northwest India region using an extended record of GRACE time-variable gravity solutions as well as simulated soil-water variations from the Global Land Data Assimilation System. Their findings indicate that groundwater was being depleted at a mean rate of 17.7 ± 4.5 km^3 per year over the Indian states of Rajasthan, Punjab and Haryana. During the study period of August 2002

to October 2008, groundwater depletion was equivalent to a net loss of 109 km^3 of water, which is double the capacity of India's largest surface-water reservoir.

Another example of the use of GRACE data for groundwater monitoring arises in a study conducted by Iqbal et al. (2016) over Pakistan. Like other agrarian countries, Pakistan is heavily dependent on its groundwater resources to meet the irrigated agricultural water demand. Iqbal et al. (2016) evaluate the potential of GRACE TWS data of changes in groundwater storage as a cost-effective approach for groundwater monitoring and sustainable water management in the Indus basin. The GRACE data from 2003 to 2010 were analyzed as total water storage variations. The VIC (variable infiltration capacity) hydrological model-generated soil moisture and surface runoff were used for the separation of TWS into groundwater storage anomalies. The GRACE-based groundwater storage anomalies are found to agree with trends inferred from in-situ ground data. A general depletion trend is observed in Upper Indus Plain where groundwater is declining at a mean rate of about 13.5 mm per year in equivalent height of water during 2003–2010. A total loss of about 11.82 km^3 per year fresh groundwater stock is inferred for Upper Indus Plain. Based on total water storage variations and ground knowledge, the two southern river plains, Bari and Rechna are found to be under threat of extensive groundwater depletion. Iqbal et al. (2016) find that the GRACE-based estimation of groundwater storage changes is skillful enough to provide monthly updates on the trend of the groundwater storage changes for resource managers and policy makers of Indus basin.

6.3 Flood Potential
Another application of TWS anomalies is in assessing flood potential (Reager et al. 2014). TWS anomalies indicate the total change in water content of a watershed. If a watershed already stores more water than "normal", this increases the likelihood of a precipitation event leading to a flood. GRACE and GRACE-FO help show how total water storage impacts the predisposition of a region to flooding, which can ultimately result in longer lead times in flood warnings. For example, Reager et al. (2014) use a case study of the catastrophic 2011 Missouri River floods to establish a relationship between river discharge, as measured by gauge stations, and basin-wide water storage, as measured remotely by GRACE. They show that the inclusion of GRACE-based total water storage information allows us to assess the predisposition of a river basin to flooding as much as 5–11 months in advance.

6.4 Drought Monitoring
As part of an effort to create a more comprehensive and objective identification of drought conditions in North America, GRACE-based drought indicators were developed. This involved integrating spatially, temporally, and vertically disaggregated GRACE terrestrial water storage (TWS) data into the U.S. and North American Drought Monitors (Houborg et al., 2012). TWS comprises the sum of the five major components of the terrestrial hydrologic cycle: groundwater, soil moisture, surface waters, snow and ice. Previously, the drought monitors lacked objective information on deep soil moisture and groundwater conditions, which are useful indicators of drought. Extensive data sets of groundwater storage from U.S. Geological Survey monitoring wells and soil moisture from the Soil Climate Analysis Network were used to assess improvements in the hydrological modeling skill resulting from the assimilation of GRACE TWS data. The results point toward modest, but statistically significant, improvements in the

hydrological modeling skill across major parts of the United States, highlighting the potential value of a GRACE-assimilated water storage field for improving drought detection. GRACE assimilation has also been demonstrated to increase correlation between TWS estimates and gauged river flow, indicating that data assimilation has considerable potential to downscale GRACE TWS data for hydrological applications (Zaitchik et al., 2008).

6.5 Ice Mass Change
GRACE plays a critical role in measuring total long-term ice mass variations. Velicogna et al. (2006) determined mass variations of the Antarctic ice sheet from 2002–2005, and found that the mass of the ice sheet decreased significantly, at a rate of 152 ± 80 cubic kilometers of ice per year, which is equivalent to 0.4 ± 0.2 millimeters of global sea level rise per year. Most of this mass loss came from the West Antarctic Ice Sheet. Velicogna et al. (2014) use GRACE to determine the regional acceleration in ice mass loss in Greenland and Antarctica for 2003–2013 and find that the total mass loss is controlled by only a few regions. In Greenland, the southeast and northwest generate 70% of the loss (280±58 Gt/yr) mostly from ice dynamics, the southwest accounts for 54% of the total in loss (25.4±1.2 Gt/yr) from a decrease in surface mass balance, followed by the northwest (34%), with no significant acceleration in the northeast. In Antarctica, the Amundsen Sea sector and the Antarctic Peninsula account for 64% and 17%, respectively, of the total loss (180±10 Gt/yr), which Velicogna et al. (2014) attribute mainly to ice dynamics.

6.6 Global and Regional Sea Level-Budget
The causes and implications of long-term global sea-Level-rise have been well established in scientific literature (IPCC *Climate Change 2013*). Sea-Level-rise is caused by a combination of freshwater increase due to the melting of land ice and "thermal expansion", which arises due to warming ocean temperatures. Since 2003, ocean temperature data for depths above 2,000 m have become available on a regular basis with the advent of the Argo array of profiling floats. Measurements from ships provide observations from earlier periods but are mostly limited to depths above 700 m. The ocean layers above 700 m and 2,000 m represent only 20% and 50%, respectively, of the total ocean volume Llovel et al. (2015).

Combining observations of sea level from altimeters with GRACE observations of ocean mass change provides a new constraint on the rate of thermal expansion in the global ocean, and hence on ocean heat content change, which enable a more complete estimation of the global sea Level-budget. For instance, Llovel et al. (2015) found that the deep-ocean (below 2000m) for the 2005-2013 period had not shown large warming and thus sea Level-trends, but the uncertainties (-0.13 ± 0.72 mm yr^{-1} to global sea-Level-rise and -0.08 ± 0.43 W m^{-2} to Earth's energy balance) are fairly large due to trend uncertainties in geocenter and GIA estimates, in particular. However, a similar sea Level-budget approach (altimetry minus GRACE and upper ocean steric signals) on a more regional Level-in the South Pacific revealed a clear deep (below 2000m) ocean warming signal (Volkov et al., 2016).

6.7 Global Water Cycle Effects on Sea Level
GRACE data has also been used to understand how the internal variability of the global water cycle contributes to sea level variations. Hamlington et al. (2017) quantify the contribution of TWS variability to sea level variability on decadal timescales. They find that decadal sea level

variability centered in the Pacific Ocean is closely tied to low frequency variability of TWS in key areas across the globe.

Reager et al. (2016) combine GRACE data with estimates of mass loss by glaciers to estimate groundwater's impact on sea-level change. Results showed that between 2002 and 2014, climate-driven variability in precipitation resulted in an additional 3200 ± 900 gigatons of water being stored on land, which caused net groundwater storage to increase. This gain slowed the rate of sea level rise by 0.71 ± 0.20 millimeters per year.

Although the rise of the global ocean has been remarkably steady for most of this time, between early 2010 and summer 2011, global sea level fell sharply, by about half a centimeter. Using data from GRACE, Boening et al. (2012) showed that the drop was caused by the very strong La Niña that began in late 2010. This periodic Pacific Ocean climate phenomenon changed rainfall patterns all over our planet, temporarily moving large amounts of water from the ocean to the continents, primarily to Australia (see Fasullo et al., 2013), northern South America and Southeast Asia. The 2011 dip did not last for very long: by mid-2012, global mean sea level not only recovered from the 5 mm it dropped in 2010-11, it resumed its long-term mean annual rise of 3.2 mm per year.

6.8 Glacial Isostatic Adjustment
The measurement of glacial isostatic adjustment (GIA) is one of the key ways in which scientists can study the Earth's mantle, ice history, global and regional sea level histories, tide-gauge data and space terrestrial geodetic measurements. When coupled with other space and terrestrial geodetic measurements, such as GPS networks and with multi-decade terrestrial gravity data, GRACE data provide new constraints on GIA and illuminate new interpretations of ice-sheet history and mantle response.

6.9 Earthquakes
GRACE and GRACE-FO data enable the observation of coseismic and postseismic gravitational changes that occur due to earthquakes with magnitude larger than about 7.5 on the Richter scale. Even at this magnitude, however, the spatial resolution of GRACE and GRACE-FO limits the direct resolution of the full signature of earthquakes (Sun and Okubo 2004; De Linage et al., 2009). The 2004 Sumatra–Andaman earthquake is one of the biggest earthquakes ever recorded, with estimates of its magnitude ranging between 9.1 and 9.3. GRACE detected the coseismic and postseismic gravity signature of the earthquake. However, the postseismic signature has a spectral content closer to the GRACE bandwidth than the coseismic signature. De Linage et al. (2009) observe a multi-year postseismic relaxation consisting of a large-scale positive gravity anomaly extending over 15° of latitude along the subduction area. Information on the postseismic relaxation is valuable in order to quantify the bulk properties of the Earth's crust and upper mantle.

6.10 Weather Forecasts
In recent years atmospheric sounding by space-based GPS radio occultation has emerged as a powerful and relatively inexpensive approach for sounding the global atmosphere with high precision, accuracy, and vertical resolution in all weather and over both land and ocean. GPS occultation is considered a valuable data source for numerical weather prediction and climate

change studies. GRACE has been used to produce this data with the radio occultation technique, which makes use of the radio signals transmitted by dedicated GPS receivers onboard GRACE. GRACE-FO continues the radio occultation measurements of atmospheric temperature and humidity profiles for use by weather service agencies.

7. LEVEL-3 DATA ACCESS, USER GUIDELINES, AND USE CASES

7.1 Data Description

Table 2 summarizes key information about GRACE-FO data, including information on the satellites' orbit as well as Level-3 data spatial resolution, temporal resolution and latency. GRACE level-3 data products are delivered in several data formats to accommodate a range of user needs. The formats are: *netcdf, ascii, geotiff* (land only).

Each monthly GRACE Tellus grid represents the surface mass deviation for that month relative to a baseline temporal average (most often 2004-2009). For comparisons against other data or models, it is critical that anomalies relative to the same time-average are compared. This is simple to do: for example, if the new baseline is 2004-2006, average the data over 1/2004 to 12/2006 for all grid points, and subtract this average grid from all other monthly grids. Please check the Frequently Asked Questions section of the GRACE Tellus website regarding other questions about the time-mean field (see https://grace.jpl.nasa.gov/about/faq/).

The mascon data are provided with a spatial sampling of 0.5 degrees in both latitude and longitude (approx. 56 km at the equator). This differs from the spherical harmonic solutions, which are provided with a spatial sampling of 1 degree in latitude and longitude. The reason for the difference is that the mascons have boundaries that lie on Parallels of approx. 0.5 degree increments. Although the grid is sampled at 0.5 degree resolution, it does not mean that two neighboring cells are 'independent' of each other. In fact, the native resolution is the size of a single mascon, which is 3 degrees (equal area) in size. The most accurate interpretation of the JPL mascon data would be obtained by summing over entire mascons using the mascon placement file (ftp://podaac.jpl.nasa.gov/allData/tellus/L3/mascon/RL05/JPL/CRI/netcdf/).

The units of the data and error grids are Liquid_Water_Equivalent_Thickness (in meter or centimeter); gain factors (scale factors) are dimensionless and time-invariant.

The grids have 720 longitude points (0.25, 0.75, 1.25, ..., 359.75), and 360 latitude points (-89.75, -89.25, ..., 89.25, 89.75).

Presently, we provide GRACE-Tellus data from the most recent GRACE gravity fields: Release 06 from CSR, JPL and GFZ. The Level-2 spherical harmonics are used as inputs to Level-3 post-processing steps. The spatial sampling of all grids is 1 degree in both latitude and longitude (approx. 111 km at the equator). However, this does not mean that two neighboring grid cells are 'independent' because (1) the actual spatial resolution of GRACE and GRACE-FO is about 330 km (Table 2), and (2) because spatial smoothing has been applied. A more detailed description of

the data processing, gain factor derivation and caveats is available in Landerer and Swenson (2012).

Orbit	
Type	Near-polar (inclination 89°)
Altitude	Approx. 356 km (Jun 2015)
In-orbit distance between GRACE 1 & 2	Approx. 200 km
Spatial Resolution	
Resolution on the ground	Approx. 330 km
Temporal Resolution	
Gravity field (Standard)	Monthly intervals
Gravity field (QuickLook)	Daily updates (over moving window covering previous 10-30 days)
Data Collection	
Latency (standard)	1-2 months
Latency (QuickLook)	3-5 days

Table 2 Overview of Level-3 relevant GRACE instrument and science measurement characteristics & constants used in this document.

The following filename convention is used:

GRD-3_[YYYYDOY-YYYYDOY]_[dddd]_[sssss]_[mmmm]_[rrvv]_[Realm]_[version]
Where:
- GRD denotes Gridded Product
- 3 denotes a GRACE Level-3 product
- [YYYYDOY-YYYYDOY] specifies the date range (in year and day-of-year format) of the data used in creating this product
- [dddd] specifies the mission
  = GRAC: Gravity Recovery and Climate Experiment
  = GRFO: Gravity Recovery and Climate Experiment Follow-On

- [sssss] is an institution specific string
  = UTCSR: The University of Texas at Austin Center for Space Research
  = JPLEM: NASA Jet Propulsion Laboratory
  = GFZOP: GFZ German Research Center for Geosciences

- [mmmm] is a 4-character mnemonic used to identify the characteristics of the gravity solution
  The 'mmmm' string is a 4-character mnemonic used to characterize the gravity solution. The first character is used to identify the primary observation type used in the gravity solution (Note: MWI = Micro Wave Instrument). The second character defines the size of the spherical harmonic expansion in the file. The third and fourth characters are used to represent other characteristics of the gravity solution, including the type of basis function used, whether it is an unconstrained or constrained solution, and the type of windowing function used. For any files that describe the average of a background model (where 'A' is

the 2nd character in the PID), only the 2nd character in the 'mmmm' string is defined/applicable. The 1st, 3rd, and 4th characters are set to be equivalent to the corresponding gravity solution.

1st Character
= A: MWI range data
= B: MWI range-rate data
= C: MWI range-acceleration data

2nd Character
= A: 60 x 60 spherical harmonic expansion
= B: 96 x 96 spherical harmonic expansion
= C: 180 x 180 spherical harmonic expansion
= D: 60 x 30 spherical harmonic expansion

3rd and 4th Characters
= 01: unconstrained spherical harmonic solution with a boxcar windowing function

- [rrvv] is a 2-digit (leading-zero-padded) release number and 2-digit (leading zeropadded) version number of underlying Level -2 product.
  The 'rrvv' string indicates the release (rr) and version (vv) of the L2 solution used for generating L3 output. The release number is tied to a specific set of background force models, and indicates consistency between solutions across different missions. All quicklook solutions will be given a release number of 'QL'. The version number indicates the version of the solution under a specific release.

- [Realm]:
  = LND (for land)
  = OCN (for ocean)
- [version]: ID to identify Level-3 processing version

In addition to the file header and name, details about the processing steps and parameters are documented in a change-log / README file for each Level-3 data product. See the Metadata File in Appendix A for a full description of each item in GRACE-FO Level-3 metadata.

7.2 Data Access

After validation, all Level-3, Level-2 and accompanying Level-1B products are released to the public through two portals. One is the Physical Oceanography Distributed Active Archive Center (PO.DAAC) at the Jet Propulsion Laboratory, Pasadena, USA, an element of the Earth Observing System Data and Information System (EOSDIS), developed by NASA. The other is the Information System and Data Center (ISDC) at GeoForschungsZentrum (GFZ) Potsdam in Germany.

As described above, the Level-3 processing is slightly different for land and ocean regions, and therefore these grids are published separately through the JPL/NASA PO.DAAC:
Ocean data: ftp://podaac-ftp.jpl.nasa.gov/allData/tellus/L3/ocean_mass/

Land data: ftp://podaac-ftp.jpl.nasa.gov/allData/tellus/L3/land_mass/

The monthly estimates are also distributed through ISDC at the **GeoForschungsZentrum Potsdam (GFZ).**

7.3 User Guidelines at a Glance

1) **Interpreting Terrestrial Water Storage Anomaly**: We assume that changes in the time-varying gravity field represent the movement of water mass over land, though this assumption should always be validated with ground data if possible. Other signals, such as tectonics, can also influence the GRACE and GRACE-FO measurements. GRACE and GRACE-FO data represent the time varying gravity field, not the static gravity field, and as such they have no mean-value by definition. In other words, GRACE and GRACE-FO data only represent anomalies with respect to the mean state (i.e. water storage anomaly) and cannot provide information about the total (absolute) amount of water stored at a location. For consistent comparisons against other data or models, the temporal mean of each dataset should be computed over a common time period and subtracted from the respective time series (as mentioned in section 7.1).

2) **Native Spatial resolution**: GRACE and GRACE-FO mass change fields can typically resolve spatial scales down to approximately 330 km. This number can vary slightly with the version being used and the smoothing that is applied during post-processing. However, the spatial sampling of the Level-3 data is often higher, with grids typically provided on a one degree (~110 km) or half-degree sampling (~55 km). Thus, users should always keep in mind that data across neighboring grid points is highly correlated and essentially a resampling of the same observation. For study areas smaller than approximately 100,000 km^2, the signal to noise ratio may be poor, and errors (especially from spatial smoothing and signal leakage, see sections 3.3.7 and 3.3.8) should be carefully assessed.

3) **Non-uniform Temporal Sampling**: the GRACE and GRACE-FO gravity fields are solved for those time periods when enough orbits exist to create a global gravity field solution. This constraint can lead to non-uniform temporal discretization of the data products when outages and breaks occur. Be careful in comparing to other data sets that the GRACE and GRACE-FO data products may not always align with calendar months, and may not be uniformly spaced in time.

4) **Error and uncertainty evaluation**: Error estimates are presented with the GRACE and GRACE-FO data products. Errors from two primary sources are calculated for spherical harmonic solutions: measurement and leakage errors. These errors should be considered, and care should be taken that these errors can be spatially correlated for regional averaging (e.g., for a river basin). Procedures and pseudo-code for averaging spatially-correlated errors are presented on the GRACE Tellus website.

5) **Available Data products**: The GRACE and GRACE-FO "mascons" (e.g. RL06M) represent the state-of-the-art in the processing of the GRACE and GRACE-FO observations to minimize signal damping and leakage errors (compared to spherical harmonic solutions). These should be used when possible, as they generally have the best signal-to-noise ratio, and lower uncertainties (see Watkins et al., 2015 or Scanlon et al., 2016 for an evaluation). For the mascon product, a

coastal resolution improvement (CRI) filter is applied to coastal mascons to reduce land signal leakage from ocean mascons. For most hydrology, cryospheric, and oceanographic applications, the CRI corrected data should be used.

6) **Gain-factors**: Model-derived gain factors (also called scale factors) are provided with the data. These can be used to enhance the spatial resolution of the GRACE observations (to 0.5 degrees for mascons, and to 1 degree for harmonic-based grids). These gain factors are derived by applying GRACE processing to model estimates of terrestrial water storage and subsequently estimating the gain factor necessary to restore the amplitude of the original model estimates. Because these gain factors rely on spatial information provided by a land surface or hydrological model, caution should be used in their interpretation as these models might have biases and typically do not include groundwater or human activities in their simulations. GRACE and GRACE-FO data for groundwater studies or studies of human impacts on hydrology may require additional, customized gain factors. The appropriate use and limitations of gain factors is discussed further in Landerer and Swenson (2012) and Long et al. (2015).

If each grid node is $g(x,y,t)$ where x is longitude index, y is latitude index, t is time index, and the gain factor is $s(x,y)$, then the gain-corrected time series is simply

$$g'(x,y,t) = g(x,y,t) * s(x,y)$$

7.4 Data Use Cases
The following use cases provide simple and easy to follow examples of how to use GRACE and GRACE-FO Level-3 data. They are designed to be accessible to new and beginner users to facilitate proper analysis and interpretation. This section is a summary of those use cases, and the step-by-step instructions are presented later in Appendices A, B, C and D.

7.4.1 Water Storage Anomalies Over the Colorado River Basin
Goal: Produce a time series and map of liquid water equivalent thickness anomalies in the Colorado (CO) River Basin.

Approach: In order to get to know GRACE Level-3 data before doing any data processing, we will first explore the data with an online interactive data plotter. Then, we will download the data and conduct the necessary pre-processing to produce a time series of Terrestrial Water Storage anomalies of the CO Basin and a map for the example time period of June, 2016.

**Summary of Steps (also see Appendix A):**
1. Explore GRACE Level-3 Terrestrial Water Storage anomalies of the CO Basin using the interactive online data plotter
2. Download Level-3 gridded Terrestrial Water Storage anomalies mascons
3. Pre-processing: multiply mascon data by gain factors
4. Create a map and time series graph of the water storage anomalies in the CO River Basin

Note that although this example aims to determine water storage anomalies, GRACE anomalies can easily be converted to rates. For example, if GRACE observed an anomaly of 20 cm over a

given study area in April and an anomaly of 10 cm in March, then the water storage change (i.e. monthly rate) would be 10 cm/mo.

Sample Products

Liquid Water Equivalent Thickness Anomalies
Colorado River Basin, June 2016   [cm]
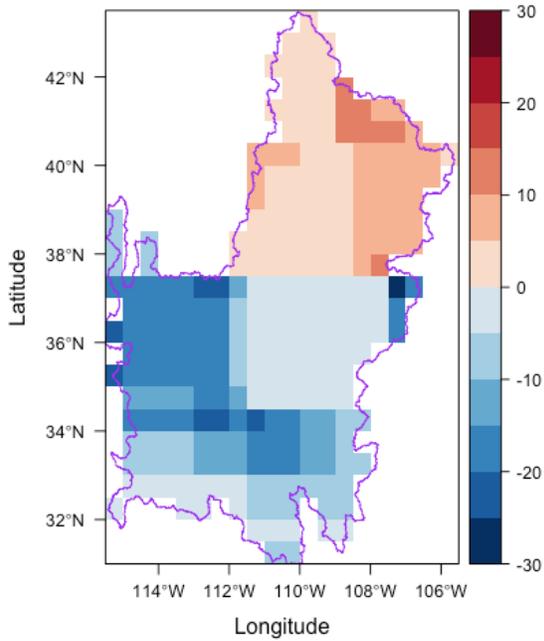
Mean Liquid Water Equivalent Thickness Anomalies
in the CO River Basin
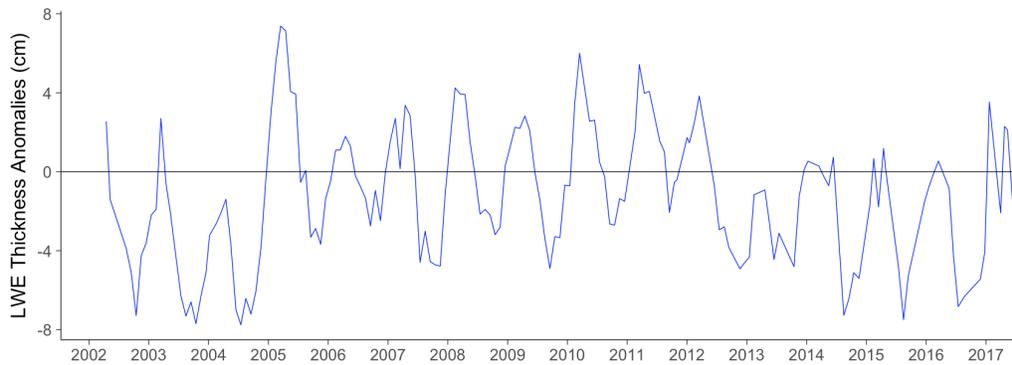
7.4.2 Groundwater Storage in the Sacramento / San Joaquin River Basin

Goal: Produce a time series of the Sacramento-San Joaquin river basin in California that shows groundwater storage anomalies from 2004 through 2015.

Approach: The basic approach to deriving groundwater anomaly estimates involves subtracting monthly anomalies of hydrologic water storage components, including soil moisture, snow water equivalent and reservoir storage, from GRACE Terrestrial Water Storage anomalies. The remaining changes in Terrestrial Water Storage can then be interpreted to result from changes in groundwater storage. However, users need to be aware that by subtracting other observations or model estimates, the remaining signal then also accumulates errors and uncertainties of those quantities as well. The approach taken here is similar to Famiglietti et al. (2011).

Summary of Steps (also see Appendix B):
1. Download the data:
    * GRACE Level-3 gridded Mascon Terrestrial Water Storage anomalies data.
    * Snow Water Equivalent from the SNOw Data Assimilation System (SNODAS)
    * Soil Moisture from the Global Land Data Assimilation System (GLDAS)
    * Reservoir storage from the California Data Exchange Center (CDEC)
    * Sacramento / San Joaquin River Basin boundary from Interactive Database of the World's River Basins
2. Pre-processing:
    * Pre-process reservoir storage anomaly data.
    * Convert all units to cm.
    * Multiply GRACE mascon data by gridded gain factors.
    * Produce anomalies for all variables of interest using the same time period as baseline as with GRACE data (Jan. 2004 – Dec. 2009).
3. Produce groundwater estimate by subtracting soil moisture, snow water equivalent, and reservoir anomalies from GRACE mascons TWS anomalies.
4. Plot the time series plot of the groundwater storage anomalies in the basin.

Sample Products

Mean Groundwater Anomalies in the Sacramento / San Joaquin River Basin
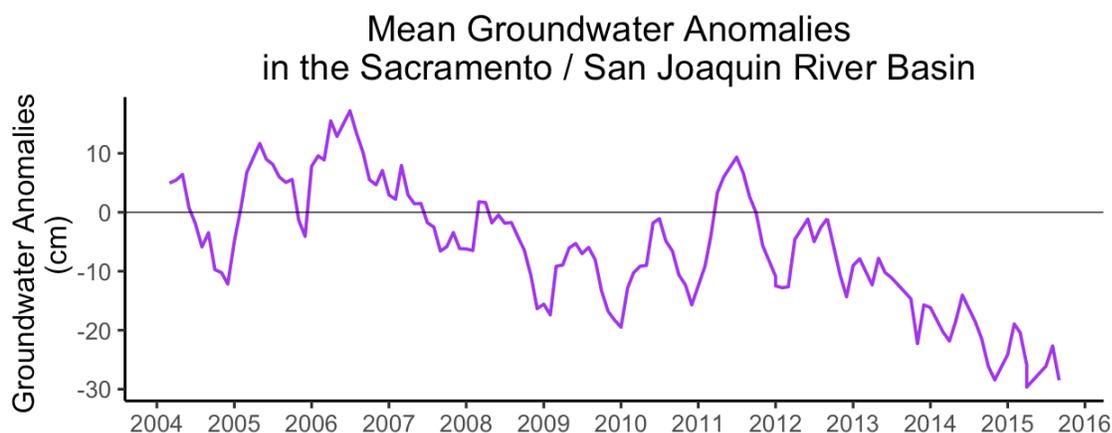
*7.4.3 Ocean Mass & Sea Level Budget*

Goal: There are two main objectives for this example. The first is to derive global ocean mass anomalies from GRACE mascon ocean bottom pressure (OBP) data. The second objective involves determining anomalies in the global sea level budget and estimate the change in ocean volume caused by thermal expansion.

Approach: The approach to derive global ocean mass anomalies involves removing the effects of atmospheric pressure from bottom pressure, and then adjusting for the difference of ocean density versus freshwater density. The resulting ocean mass anomalies are then subtracted from the sea surface height anomalies from altimetry measurements in order to assess ocean height changes caused by thermal expansion. Methods used in this use case follow those described by Llovel et al. (2015).

Summary of Steps (also see Appendix C):
1. Download the data:
   - Level-3 gridded Mascon Water Storage anomalies data from GRACE Tellus website
   - Ocean mask from GRACE Tellus website
   - GAD product from Atmosphere and Ocean Dealiasing Level-1B (AOD1B). GAD represents the bottom pressure simulated by Ocean Model for Circulation and Tides (OMCT), forced by atmospheric energy and momentum fluxes (e.g., wind stress). In this application, only the global ocean mean of GAD is required.
   - Global GIA-corrected Sea Level-time series.
2. Convert GRACE ocean bottom pressure (OBP) mascons to ocean mass anomalies:
   - Apply ocean mask to isolate the ocean in GRACE mascons
   - Remove effect of atmospheric pressure by subtracting the GAD background model from GRACE mascons
   - Obtain ocean mass anomalies by adjusting for the difference in ocean density versus freshwater density (a small correction)
3. Use a sea level budget approach to estimate thermal expansion
   - Subtract sea surface height from ocean mass anomalies.
   - Produce a graph and time series decomposition of the component of ocean height change attributed to thermal expansion.

Sample Product
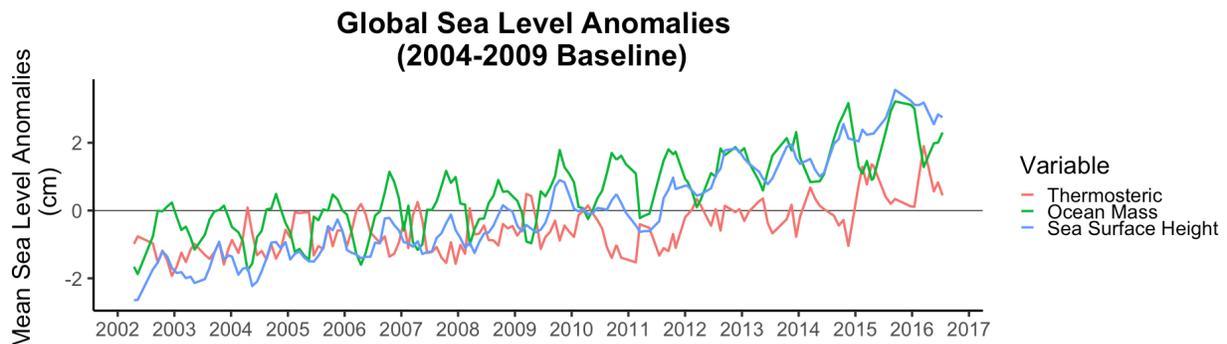
7.4.4 Ocean Currents & Transport

Goal: The goal of this use case is to summarize the steps taken by Landerer et al. (2015), who present the first measurements of changes in the meridional transport of large-scale Atlantic Meridional Overturning Circulation (AMOC) flows using Ocean Bottom Pressure (OBP) estimates derived from GRACE.

Approach: The methodology involves using the zonal OBP differences at the basin boundaries of the Atlantic to obtain information on AMOC variations. As the large-scale flows are dominated by a geostrophic balance, the meridional transport per unit depth at a particular latitude and depth can be derived from the zonal bottom pressure differences and at the eastern and western basin boundaries. Methods for this use case are described in detail by Landerer et al. (2015).

Summary of Steps (also see Appendix D):
1. Download the data:
    a. Level-3 gridded Mascon Terrestrial Water Storage anomalies data from GRACE Tellus website
    b. Ocean mask from GRACE Tellus website
2. Use GRACE ocean bottom pressure (OBP) mascons to characterize AMOC variations.
    a) Derive the meridional transport $T(y, z)$ at a particular latitude (y) and depth (z) by dividing the zonal bottom pressure differences $P_E\ (y, z)$ and $P_W\ (y, z)$ at the eastern and western basin boundaries by the Coriolis parameter (f) and the mean sea water density (ρ_0):

$$T(y, z) = \frac{P_E\ (y, z) - \ P_W\ (y, z)}{\rho_0 f}$$

    b) Integrating this between depth levels $z1$ and $z2$ yields the layer geostrophic AMOC volume transport from ocean bottom pressure data across the ocean basin:

$$T(y) = \frac{1}{\rho_0 f} \int_{z1}^{z2} P_E\ (y, z) - \ P_W\ (y, z)\ dz$$

Sample Products
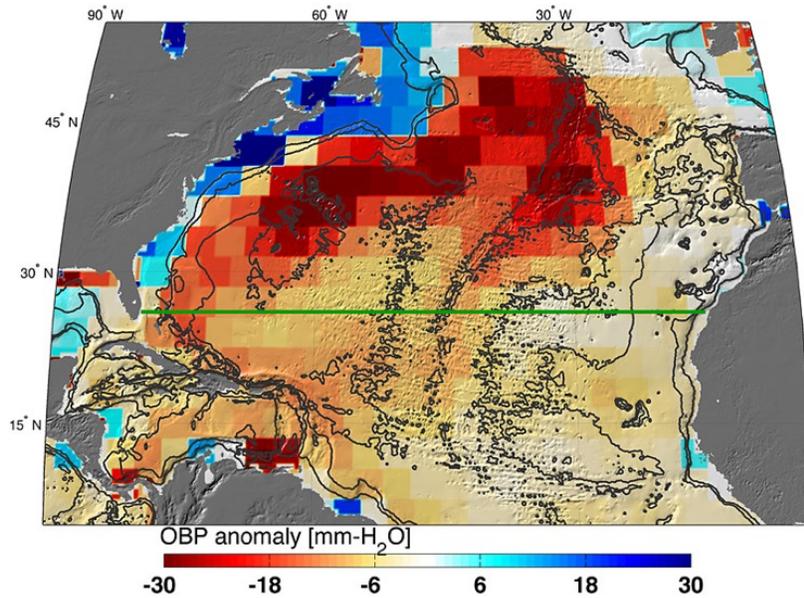
Figure 5 The map shows ocean bottom pressure anomalies (mean of November 2009 through March 2010, relative to 2005–2012 mean) over the North Atlantic basin. Also shown is the location of the hydrographic in situ RAPID MOCHA section (green line; *Marotzke et al.*, 2002). Bottom pressure signals are largest on the western side of the basin and tend to be anticorrelated between shallow (0–1000 m) and deeper ocean regions (1000–5000 m) (see also Figure 1). One mm-H_2O OBP corresponds to approximately 10 Pa. Figure from Landerer et al. (2015).
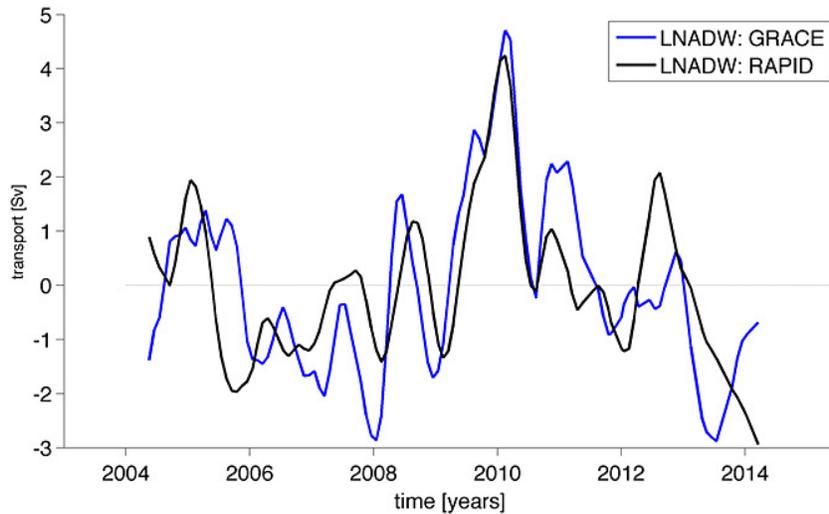
Figure 6 The graph shows meridional transport estimates from GRACE OBP anomalies on the eastern and western margin integrated over the 3000–5000 m depth layer at 26.5N, compared to the RAPID-MOCHA estimate of LNADW. The RMS difference between these two estimates is 1.2 Sverdrup and the correlation is R = 0.69. The 1 sigma error of the GRACE-LNADW estimate is ±1.1 Sverdrup. Figure from Landerer et al. (2015).

REFERENCES

Bertiger, W., Dunn, C., Harris, I., Kruizinga, G., Romans, L., Watkins, M., and Wu, S. (2003). "Relative Time and Frequency Alignment between Two Low Earth Orbiters", *Proceedings of Institute of Electrical and Electronics Engineers Conference*, Frequency Control Symposium, Tampa, FL.

Boening, C., Willis, J. K., Landerer, F. W., Nerem, R. S., & Fasullo, J. (2012). The 2011 La Niña: So strong, the oceans fell. *Geophysical Research Letters*, *39*(19).

Chambers, D. P. (2006). Evaluation of new GRACE time-variable gravity data over the ocean. *Geophysical Research Letters*, *33*(17).

Chambers, D. P., & Willis, J. K. (2010). A global evaluation of ocean bottom pressure from GRACE, OMCT, and steric-corrected altimetry. *Journal of Atmospheric and Oceanic Technology*, *27*(8), 1395-1402.

Chambers, D. P., & Bonin, J. A. (2012). Evaluation of Release-05 GRACE time-variable gravity coefficients over the ocean. *Ocean Science*, *8*(5), 859-868.

Cheng, M. K., Ries, J. C., & Tapley, B. D. (2013). Geocenter variations from analysis of SLR data. In *Reference frames for applications in geosciences* (pp. 19-25). Springer, Berlin, Heidelberg.

Cheng, M., Tapley, B. D., & Ries, J. C. (2013). Deceleration in the Earth's oblateness. *Journal of Geophysical Research: Solid Earth*, *118*(2), 740-747.

Cheng, M., Ries, J. C., & Tapley, B. D. (2011). Variations of the Earth's figure axis from satellite laser ranging and GRACE. *Journal of Geophysical Research: Solid Earth*, *116*(B1).

Cox, C. M., & Chao, B. F. (2002). Detection of a large-scale mass redistribution in the terrestrial system since 1998. *Science*, *297*(5582), 831-833.

De Linage, C., Rivera, L., Hinderer, J., Boy, J. P., Rogister, Y., Lambotte, S., & Biancale, R. (2009). Separation of coseismic and postseismic gravity changes for the 2004 Sumatra–Andaman earthquake from 4.6 yr of GRACE observations and modelling of the coseismic change by normal-modes summation. *Geophysical Journal International*, *176*(3), 695-714.

Decadal Survey for Earth Science and Applications from Space (ESAS, 2017). The National Academies of Sciences, Engineering, and Medicine. Retrieved from: http://sites.nationalacademies.org/DEPS/ESAS2017/

Duan, X. J., Guo, J. Y., Shum, C. K., & Van Der Wal, W. (2009). On the postprocessing removal of correlated errors in GRACE temporal gravity field solutions. *Journal of Geodesy*, *83*(11), 1095.

Famiglietti, J. S., Lo, M., Ho, S. L., Bethune, J., Anderson, K. J., Syed, T. H., ... & Rodell, M. (2011). Satellites measure recent rates of groundwater depletion in California's Central Valley. *Geophysical Research Letters*, *38*(3).

Fasullo, J. T., Boening, C., Landerer, F. W., & Nerem, R. S. (2013). Australia's unique influence on global sea level in 2010–2011. *Geophysical Research Letters*, *40*(16), 4368-4373.

Flechtner, F., Dobslaw, H., Fagiolini, E. (2015). "AOD1B Product Description Document", Rev 4.4, GRACE 327-750. Gravity Recovery and Climate Experiment. Retrieved from http://wwwapp2.gfzpotsdam.de/pb1/op/grace/results/grav/AOD1B_20151214.pdf.

Ghobadi-Far, K., Sprlak, M., & Han, S.-C. (2019), Determination of ellipsoidal surface mass change from GRACE time-variable gravity data, Geophysical Journal International, 219(1), 248-259. 10.1093/gji/ggz292.

Hamlington, B. D., Reager, J. T., Lo, M. H., Karnauskas, K. B., & Leben, R. R. (2017). Separating decadal global water cycle variability from sea level rise. *Scientific reports*, *7*(1), 995.

Hardy, R. A., Nerem, R. S., & Wiese, D. N. (2017). The Impact of Atmospheric Modeling Errors on GRACE Estimates of Mass Loss in Greenland and Antarctica. *Journal of Geophysical Research: Solid Earth*, *122*(12).

Heiskanen, W. A., & Moritz, H. (1967). Physical geodesy. *Bulletin Géodésique (1946-1975)*, *86*(1), 491-492.

Houborg, R., Rodell, M., Li, B., Reichle, R., & Zaitchik, B. F. (2012). Drought indicators based on model-assimilated Gravity Recovery and Climate Experiment (GRACE) terrestrial water storage observations. *Water Resources Research*, *48*(7).

Intergovernmental Panel on Climate Change (2013), *Climate Change 2013: The Physical Science Basis, Contribution of Working Group I to the Fifth Assessment Report of the Intergovernmental Panel on Climate Change*, edited by Stocker T. F., 1535 pp., Cambridge Univ. Press, Cambridge, U. K., and New York, doi:10.1017/CBO9781107415324.

Iqbal, N., Hossain, F., Lee, H., & Akhter, G. (2016). Satellite gravimetric estimation of groundwater storage variations over Indus Basin in Pakistan. *IEEE Journal of Selected Topics in Applied Earth Observations and Remote Sensing*, *9*(8), 3524-3534.

Jacob, T., Wahr, J., Pfeffer, W. T., & Swenson, S. (2012). Recent contributions of glaciers and ice caps to sea level rise. *Nature*, *482*(7386), 514.

Khan, S. A., Kjaer, K. H., Korsgaard, N. J., Wahr, J., Joughin, I. R., Timm, L. H., ... & Csatho, B. M. (2013). Recurring dynamically induced thinning during 1985 to 2010 on Upernavik Isstrøm, West Greenland. *Journal of Geophysical Research: Earth Surface*, *118*(1), 111-121.

Landerer, F. W., & Swenson, S. C. (2012). Accuracy of scaled GRACE terrestrial water storage estimates. *Water resources research*, *48*(4).

Landerer, F. W., Wiese, D. N., Bentel, K., Boening, C., & Watkins, M. M. (2015). North Atlantic meridional overturning circulation variations from GRACE ocean bottom pressure anomalies. *Geophysical Research Letters*, *42*(19), 8114-8121.

Llovel, W., Willis, J. K., Landerer, F. W., & Fukumori, I. (2014). Deep-ocean contribution to sea level and energy budget not detectable over the past decade. *Nature Climate Change, 4*(11), 1031.

Long, D., Longuevergne, L., & Scanlon, B. R. (2015). Global analysis of approaches for deriving total water storage changes from GRACE satellites. *Water Resources Research*, 51(4), 2574-2594.

Longuevergne, L., Wilson, C., Scanlon, B. R., & Crétaux, J. F. (2013). GRACE water storage estimates for the Middle East and other regions with significant reservoir and lake storage. *Hydrology and Earth System Sciences*, *17*(12), 4817-4830.

Luthcke, S. B., Sabaka, T. J., Loomis, B. D., Arendt, A. A., McCarthy, J. J., & Camp, J. (2013). Antarctica, Greenland and Gulf of Alaska land-ice evolution from an iterated GRACE global mascon solution. *Journal of Glaciology, 59*(216), 613-631.

Marotzke, J., S. A. Cunningham, and H. L. Bryden (2002), Monitoring the Atlantic Meridional Overturning Circulation at 26.5°N. *Southampton Oceanography Centre*, Southampton, U. K.

Marshall, J., Adcroft, A., Hill, C., Perelman, L., & Heisey, C. (1997). A finite-volume, incompressible Navier Stokes model for studies of the ocean on parallel computers. Journal of Geophysical Research: *Oceans, 102*(C3), 5753-5766.

Morison, J., Wahr, J., Kwok, R., & Peralta-Ferriz, C. (2007). Recent trends in Arctic Ocean mass distribution revealed by GRACE. *Geophysical Research Letters*, *34*(7).

Park, J. H., Watts, D. R., Donohue, K. A., & Jayne, S. R. (2008). A comparison of in situ bottom pressure array measurements with GRACE estimates in the Kuroshio Extension. *Geophysical Research Letters*, *35*(17).

Peltier, W. R., Argus, D. F., & Drummond, R. (2015). Space geodesy constrains ice age terminal deglaciation: The global ICE-6G_C (VM5a) model. *Journal of Geophysical Research: Solid Earth*, *120*(1), 450-487.

Peralta-Ferriz, C., Morison, J. H., Wallace, J. M., Bonin, J. A., & Zhang, J. (2014). Arctic Ocean circulation patterns revealed by GRACE. *Journal of Climate*, *27*(4), 1445-1468.

Ponte, R. M., Quinn, K. J., Wunsch, C., & Heimbach, P. (2007). A comparison of model and GRACE estimates of the large-scale seasonal cycle in ocean bottom pressure. *Geophysical research letters*, *34*(9).

Quinn, K. J., & Ponte, R. M. (2010). Uncertainty in ocean mass trends from GRACE. *Geophysical Journal International*, *181*(2), 762-768.

Reager, J. T., Thomas, B. F., & Famiglietti, J. S. (2014). River basin flood potential inferred using GRACE gravity observations at several months lead time. *Nature Geoscience, 7*(8), 588.

Reager, J. T., Gardner, A. S., Famiglietti, J. S., Wiese, D. N., Eicker, A., & Lo, M. H. (2016). A decade of sea level rise slowed by climate-driven hydrology. *Science, 351*(6274), 699-703.

Reese, C. C., Solomatov, V. S., & Baumgardner, J. R. (2002). Survival of impact-induced thermal anomalies in the Martian mantle. *Journal of Geophysical Research: Planets, 107*(E10).

Rietbroek, R., LeGrand, P., Wouters, B., Lemoine, J. M., Ramillien, G., & Hughes, C. W. (2006). Comparison of in situ bottom pressure data with GRACE gravimetry in the Crozet-Kerguelen region. *Geophysical research letters*, *33*(21).

Rodell, M., Velicogna, I., & Famiglietti, J. S. (2009). Satellite-based estimates of groundwater depletion in India. *Nature, 460*(7258), 999.

Rodell, M., Famiglietti, J. S., Wiese, D. N., Reager, J. T., Beaudoing, H. K., Landerer, F. W., & Lo, M. H. (2018). Emerging trends in global freshwater availability. *Nature*, 1.

Rowlands, D. D., Luthcke, S. B., McCarthy, J. J., Klosko, S. M., Chinn, D. S., Lemoine, F. G., ... & Sabaka, T. J. (2010). Global mass flux solutions from GRACE: A comparison of parameter estimation strategies—Mass concentrations versus Stokes coefficients. *Journal of Geophysical Research: Solid Earth, 115*(B1).

Sakumura, C., Bettadpur, S., & Bruinsma, S. (2014). Ensemble prediction and intercomparison analysis of GRACE time-variable gravity field models. *Geophysical Research Letters*, *41*(5), 1389-1397.

Scanlon, B. R., Zhang, Z., Save, H., Wiese, D. N., Landerer, F. W., Long, D., ... & Chen, J. (2016). Global evaluation of new GRACE mascon products for hydrologic applications. *Water Resources Research*, 52(12), 9412-9429.

Scanlon, B. R., Zhang, Z., Save, H., Sun, A. Y., Schmied, H. M., van Beek, L. P., ... & Longuevergne, L. (2018). Global models underestimate large decadal declining and rising water storage trends relative to GRACE satellite data. *Proceedings of the National Academy of Sciences*, 201704665.

Smeed, D.A., McCarthy, G., Cunningham, S.A., Frajka-Williams, E., Rayner, D., Johns, W.E., Meinen, C.S., Baringer, M.O., Moat, B.I., Duchez, A. and Bryden, H.L., 2014. Observed decline of the Atlantic meridional overturning circulation 2004–2012. Ocean Science, 10(1), pp.29-38.
Sun, W., & Okubo, S. (2004). Truncated co-seismic geoid and gravity changes in the domain of spherical harmonic degree. *Earth, planets and space, 56*(9), 881-892.

Swenson, S., Chambers, D., & Wahr, J. (2008). Estimating geocenter variations from a combination of GRACE and ocean model output. *Journal of Geophysical Research: Solid Earth*, *113*(B8).

Swenson, S., and J. Wahr (2006), Post-processing removal of correlated errors in GRACE data, *Geophysical Research Letters, 33*(L08402), doi:10.1029/ 2005GL025285.

Velicogna, I., and J. Wahr (1999). Are Analyzed Pressure Fields Good Enough For Geodetic Applications. *Eos Transactions, American Geophysical Union, 80*(46).

Velicogna, I., & Wahr, J. (2013). Time-variable gravity observations of ice sheet mass balance: Precision and limitations of the GRACE satellite data. *Geophysical Research Letters, 40*(12), 3055-3063.

Velicogna, I., Sutterley, T. C., & Van Den Broeke, M. R. (2014). Regional acceleration in ice mass loss from Greenland and Antarctica using GRACE time-variable gravity data. *Geophysical Research Letters, 41*(22), 8130-8137.

Wahr, J., Molenaar, M., & Bryan, F. (1998). Time variability of the Earth's gravity field: Hydrological and oceanic effects and their possible detection using GRACE. *Journal of Geophysical Research: Solid Earth, 103*(B12), 30205-30229.

Wang, F. (2000). Grace CG Offset Determination by Magnetic Torquers During the In-Flight Phase. The University of Texas at Austin/Center for Space Research, Technical Memorandum, CSR-TM-00-01.

Watkins, M. M., Yuan, D., Kuang, D., Bertiger, W., Kim, M., & Kruizinga, G. L. (2005, December). GRACE harmonic and mascon solutions at JPL. In AGU Fall Meeting Abstracts. De Linage, C., Rivera, L., Hinderer, J., Boy, J. P., Rogister, Y., Lambotte, S., & Biancale, R. (2009). Separation of coseismic and postseismic gravity changes for the 2004 Sumatra–Andaman earthquake from 4.6 yr of GRACE observations and modelling of the coseismic change by normal-modes summation. *Geophysical Journal International*, *176*(3), 695-714.

Watkins, M. M., Wiese, D. N., Yuan, D. N., Boening, C., & Landerer, F. W. (2015). Improved methods for observing Earth's time variable mass distribution with GRACE using spherical cap mascons. *Journal of Geophysical Research: Solid Earth*, *120*(4), 2648-2671.

Wu, X., M. M. Watkins, R. Kwok, E. R. Ivins, P. Wang, and J. Wahr (1999). GRACE Gravity and Surface Mass Variations- Toward a Global Solution, *Eos Transactions, American Geophysical Union, 80*(46).

Zaitchik, B. F., Rodell, M., & Reichle, R. H. (2008). Assimilation of GRACE terrestrial water storage data into a land surface model: Results for the Mississippi River basin. *Journal of Hydrometeorology*, *9*(3), 535-548.

ABBREVIATIONS AND ACRONYMS

Atmosphere and Ocean De-aliasing Level-1B Product (AOD1B)

Center for Space Research at University of Texas, Austin (CSR)

Coastal Resolution Improvement (CRI)

Equivalent Water Height (EWH)

European Centre for Medium-Range Weather Forecasts (ECMWF)

German Research Centre for Geosciences / GeoforschungsZentrum Potsdam (GFZ)

Glacial Isostatic Adjustment (GIA)

Global Land Data Assimilation System (GLDAS)

Global Positioning System (GPS)

Gravity Recovery and Climate Experiment (GRACE)

Gravity Recovery and Climate Experiment Follow-On (GRACE-FO)

GRACE Data Release 05 (RL05)

Jet Propulsion Laboratory (JPL)

Mass Concentration Unit (Mascons)

Ocean Model for Circulation and Tides (OMCT)

Ocean Bottom Pressure (OBP)

Science Data System (SDS)

Terrestrial Water Storage (TWS)

ultra-stable oscillators (USO)

APPENDIX A: WATER STORAGE ANOMALIES OVER THE COLORADO RIVER BASIN

Step 1

a) Launch the interactive web application to explore GRACE anomalies located at
    https://grace.jpl.nasa.gov/data/data-analysis-tool/
b) Look at the water equivalent thickness (GRACE JPL) mascon solutions globally (Figure 1A).
c) Change the date of the data shown to see the changes in monthly water equivalent thickness anomalies.
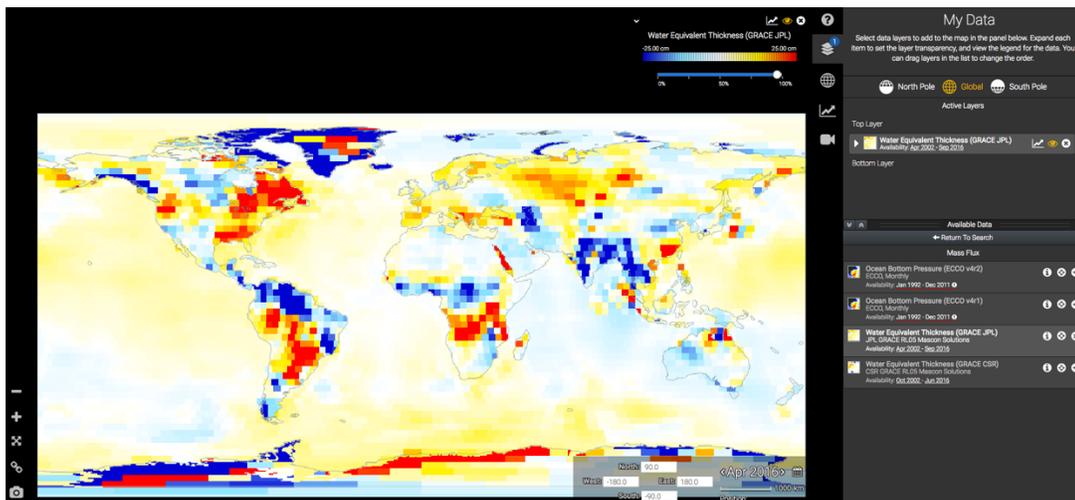
Figure 1A. Display of the interactive web application to explore GRACE data.

d) Pick a basin of interest to look at the "Analysis" output. Hover the mouse over the basin of choice and zoom in toward this location. Information on the basin area, length, continent, ocean and sea basin will appear in a pop-up box (Figure 1B).
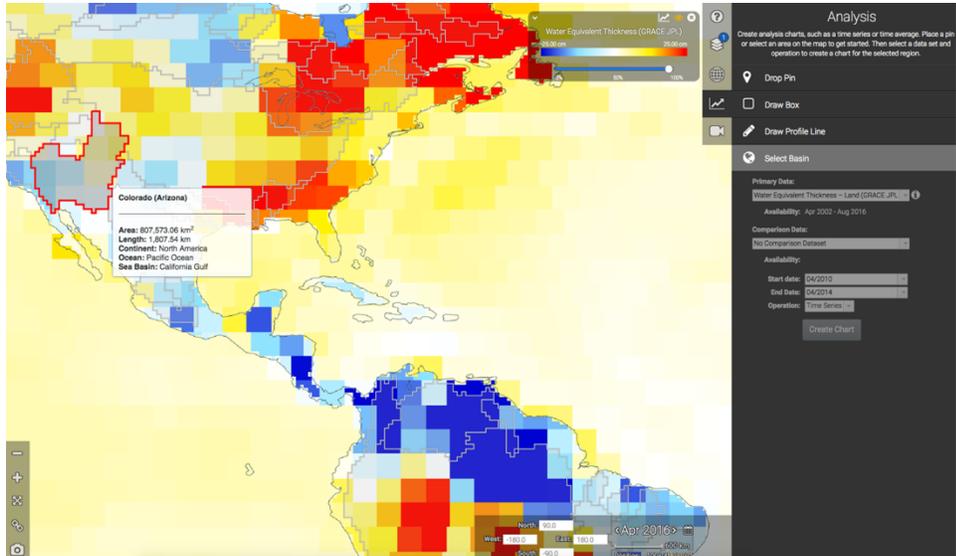
Figure 1B. Display of the interactive web application zoomed-in to the Colorado River Basin, showing information on the basin area, length, continent, ocean and sea basin in a pop-up box.

e)   Create a time series chart by specifying a start date and end date then clicking the "Create Chart" button (Figure 1C)
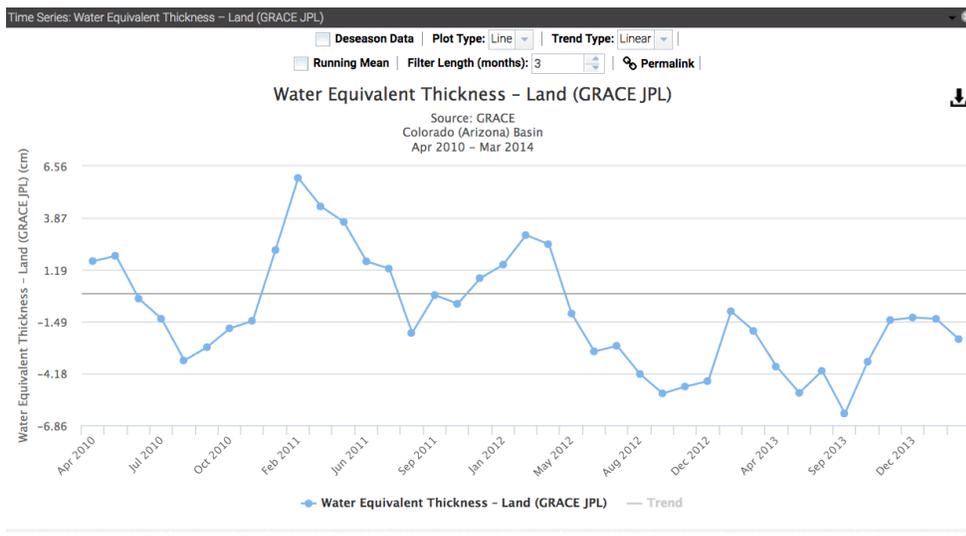
Figure 1C. Display of the interactive web application chart of Water Equivalent Thickness anomalies over the Colorado River Basin.

Step 2

f)   Download Level-3 gridded mascon Terrestrial Water Storage anomalies data from GRACE Tellus via ftp (ftp://podaac.jpl.nasa.gov/allData/tellus/L3/mascon/). We will use the Mascon dataset with the Coastline Resolution Improvement (CRI) filter (Figure 1D).

← → C ⓘ ftp://podaac.jpl.nasa.gov/allData/tellus/L3/mascon/RL05/JPL/CRI/netcdf/

Index of /allData/tellus/L3/mascon/RL05/JPL/CRI/netcdf/

[parent directory]

Name	Size	Date Modified
CLM4.SCALE_FACTOR.JPL.MSCNv01CRIv01.nc	2.0 MB	9/10/15, 5:00:00 PM
CLM4.SCALE_FACTOR.JPL.MSCNv01CRIv01.nc.md5	73 B	9/10/15, 5:00:00 PM
GRCTellus.JPL.200204_201706.GLO.RL05M_1.MSCNv02CRIv02.nc	645 MB	9/28/17, 12:36:00 PM
GRCTellus.JPL.200204_201706.GLO.RL05M_1.MSCNv02CRIv02.nc.md5	90 B	9/28/17, 12:36:00 PM
JPL_MSCNv01_PLACEMENT.nc	0 B	9/10/15, 5:00:00 PM
LAND_MASK.CRIv01.nc	2.0 MB	9/10/15, 5:00:00 PM
LAND_MASK.CRIv01.nc.md5	54 B	9/10/15, 5:00:00 PM
README.txt	940 B	11/9/15, 4:00:00 PM

Figure 1D. List of the Level-3 global mass concentration Terrestrial Water Storage anomalies derived from GRACE and GRACE-FO. This use case requires the gain factor netCDF file as well as the Coastline Resolution Improvement (CRI) filter netCDF file (highlighted by the red box).

g) Click on the README.txt for a description of the directory contents. Then click to download:
   - CLM4.SCALE_FACTOR.JPL.MSCNv01CRIv01.nc
     o Ancillary data file containing the requisite gain factor information in netCDF format required to read and process the Tellus Mascon Earth Science Data Record (ESDR).
   - GRCTellus.JPL.200204_201706.GLO.RL05M_1.MSCNv02CRIv02.nc
     o CRI-filtered Tellus Mascon Earth Science Data Record in netCDF format
h) Download the boundary shapefile for the CO River Basin (found at http://riverbasins.wateractionhub.org/)

Step 3

i) Produce a map showing the raw Level-3 CRI-filtered Liquid Water Equivalent Thickness anomalies with world countries outlined and the CO River Basin highlighted (Figure 1E).
   - NOTE: If your application requires a different baseline (e.g., instead of 2004-2009 you need 2005-2010), you can simply compute that by averaging each grid point over the 2005-2010 baseline, and subtract that value from all time steps.
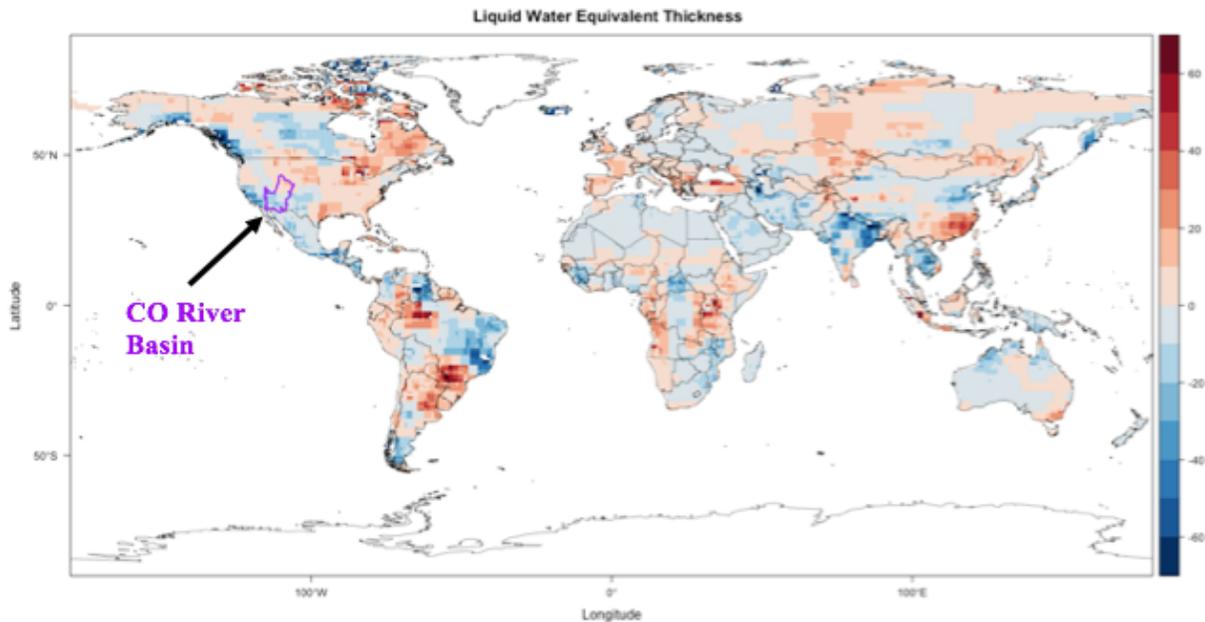
Figure 1E. Map of the raw Level-3 CRI-filtered Liquid Water Equivalent Thickness anomalies with world countries outlined and the CO River Basin highlighted.

j) Multiply the GRACE Level-3 Mascon raster by gain factor raster.
    - Due to the sampling and post-processing of GRACE observations, surface mass variations at small spatial scales tend to be attenuated. Therefore, users have the option to multiply GRACE Tellus Land data by the provided gridded gain factors.
    - The scaling grid is a set of scaling coefficients, one for each 1 degree bin of the land grids, and are intended to restore much of the signal amplitude removed by the destriping, Gaussian, and degree 60 filters applied to the land grids. To use these scaling coefficients, the time series at one grid (1 degree bin) location must be multiplied by the scaling factor at the same 1 degree bin position.
k) Subset the GRACE Mascon data to include only the CO River Basin.
l) Compare the difference in the data of the original raw data to the data corrected with the gain factors (Figure 1F).
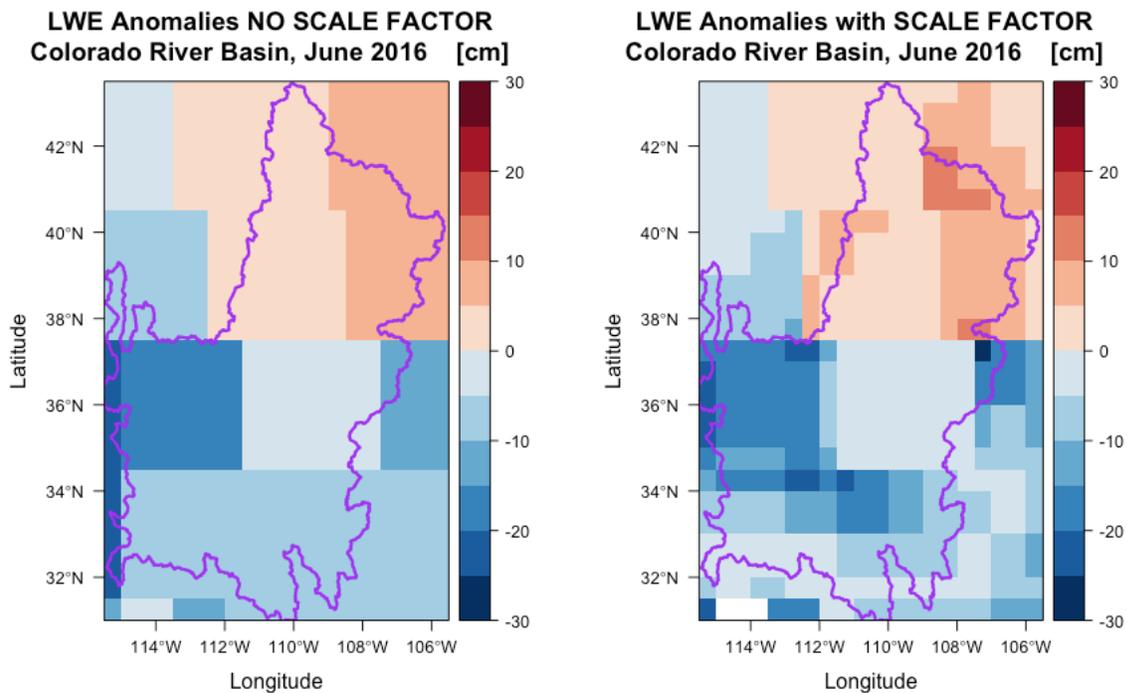
Figure 1F. GRACE Mascon water storage anomalies for June, 2016 with no gridded gain factors applied (left) and multiplied by the gridded gain factors (right).

Step 4

    m) Plot the final map of GRACE Mascon water storage anomalies for June, 2016.

    n) Then, create the time series plot showing LWE Thickness Anomalies averaged over the CO River Basin (Figure 1G).
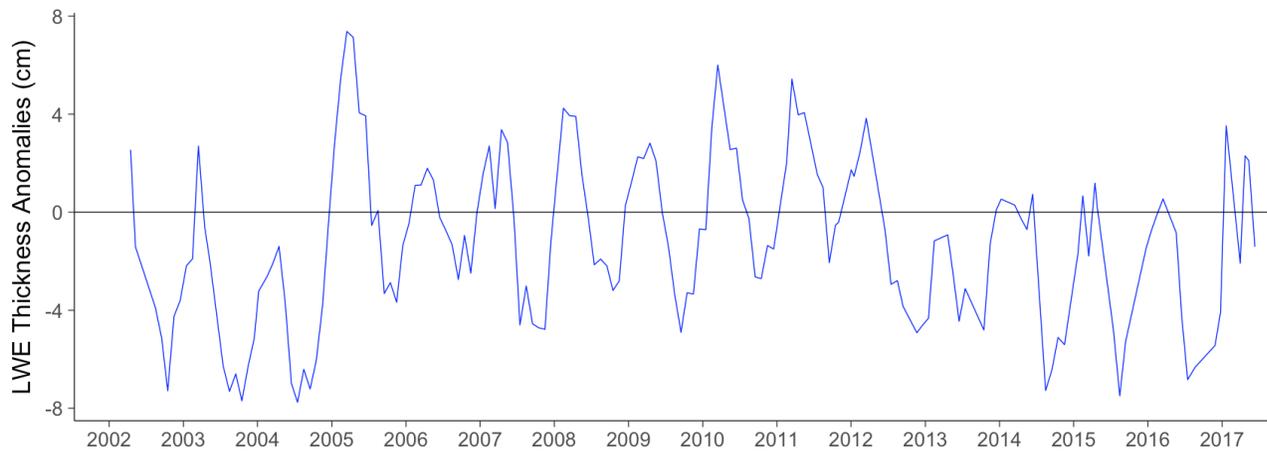
Figure 1G. GRACE Mascon Liquid Water Equivalent anomalies for June, 2016 in the CO River Basin with gain factor applied and values spatially disaggregated (top) and a time series plot showing Liquid Water Equivalent anomalies averaged over the CO River Basin.

APPENDIX B: GROUNDWATER STORAGE ANOMALIES IN THE SACRAMENTO / SAN JOAQUIN RIVER BASIN

Step 1

a) Download Level-3 gridded Coastal Resolution Improvement (CRI) filtered Mascon Terrestrial Water Storage anomalies data from GRACE Tellus (please see Water Storage Anomalies in the Colorado River Basin use case in Appendix A for details)

b) Download the boundary of the Sacramento / San Joaquin basin from Interactive Database of the World's River Basins at http://riverbasins.wateractionhub.org/ (Figure 2A).
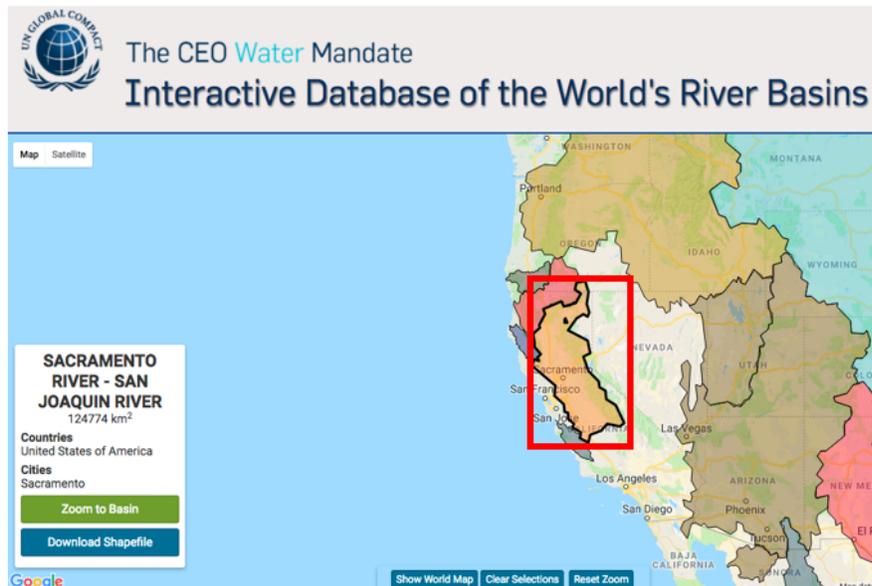
Figure 2A. The Sacramento / San Joaquin basin from Interactive Database of the World's River Basins is highlighted in red and can be downloaded as a shapefile on the lower left part of the screen.

c) Download Soil moisture from Global Land Data Assimilation System (GLDAS) at https://disc.sci.gsfc.nasa.gov/datasets?keywords=GLDAS. This example uses data from the NOAH monthly 0.125 degree resolution product (NLDAS_NOAH0125_M.002) (Figure 2B).
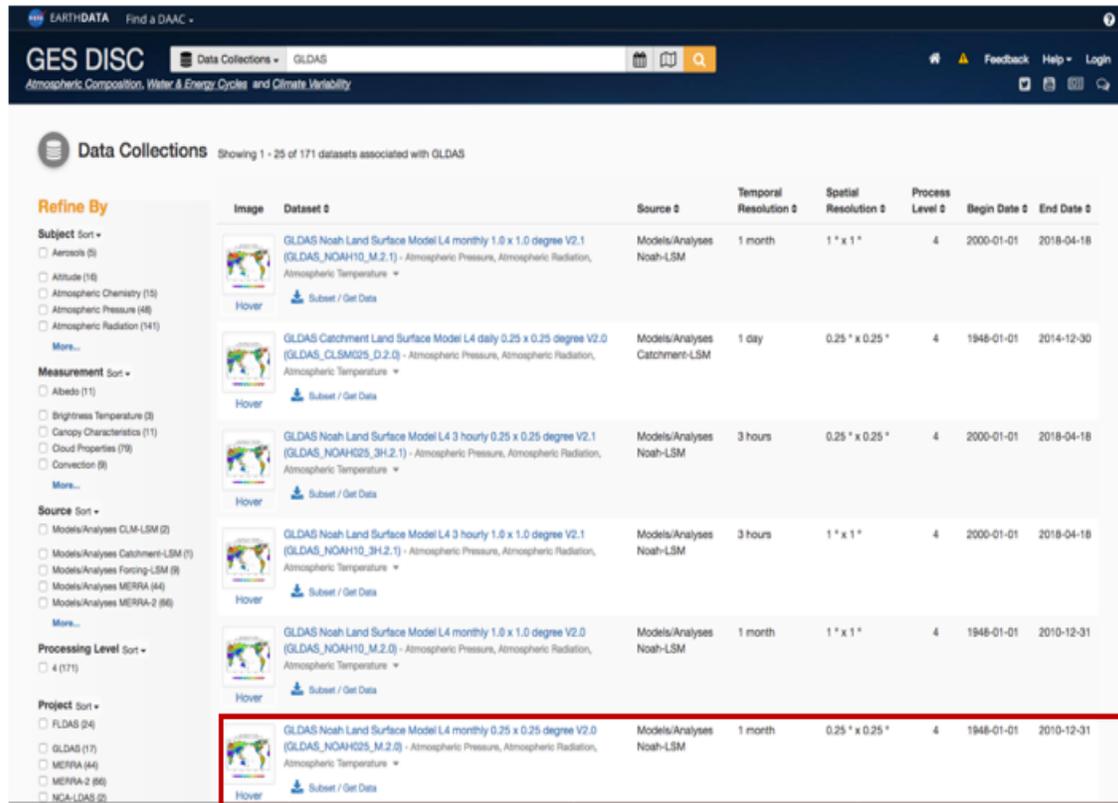
Figure 2B. The Soil moisture from Global Land Data Assimilation System (GLDAS) is highlighted in red and can be subset and downloaded in multiple raster formats.

d) Download snow water equivalent (SWE) data from SNODAS website at https://nsidc.org/data/g02158 (Figure 2C).
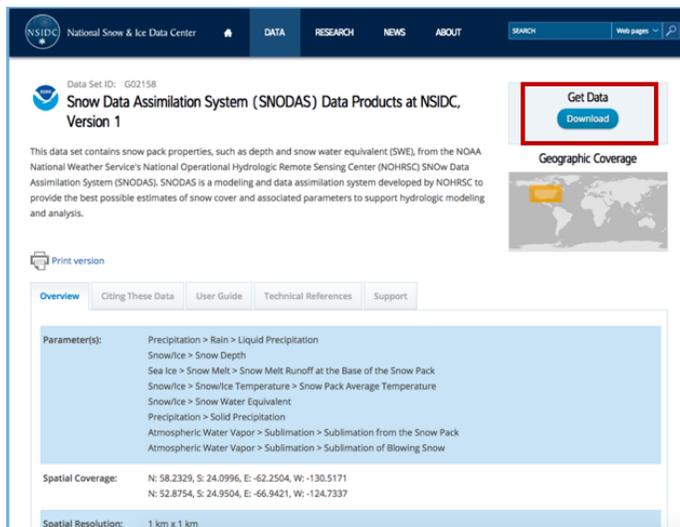
Figure 2C. The place to download Snow Water Equivalent from the SNOw Data Assimilation System (SNODAS) is highlighted in red and can be subset and downloaded in multiple raster formats.

e) Download all of the monthly reservoir level data for the time period of interest (2004 – 2015) from California Data Exchange Center (CDEC) at https://cdec.water.ca.gov (Figure 2D).

f) Subset the stations with latitude and longitude coordinates that fall into the study area boundary.

Figure 2D. The California Data Exchange Center (CDEC) hosts the Reservoir level data used for this use case.

Step 2

g) Convert tabular reservoir storage anomaly data to raster data and conduct the unit conversions.

    i. Convert the tabular data to point data using the latitude and longitude information from each reservoir measurement station.

    ii. Create a raster from each reservoir station point. The spatial resolution of the resulting raster pixels should equal the spatial resolution of the GRACE data (0.5 degrees).

    iii. We need to end up with all input data using the same units of measurement. In this example, we choose to use cm to match GRACE LWE thickness units.

- First, convert acre-feet to km^3 by multiplying each cell in the raster by 0.000001233.
- To account for the area of the pixel, (which is 0.5 degrees x 0.5 degrees = ~55.5km x 55.5km), divide each raster cell by $(55.5km)^2 = 3080.25km^2$
- Multiply the raster by 100,000 to convert the height in kilometers to centimeters.

h) Conduct the unit conversions for soil moisture and snow water equivalent.

    i. For soil moisture, we need to convert the original units of $[kg/m^2]$ to $[cm]$.

       ○ 1 [kg] of water at Standard Temperature and Pressure = 1 [liter] = 1000 $[cm^3]$.

       ○ 1 $[m^2]$ = 10,000 $[cm^2]$.

       ○ Therefore, 1 $[kg/m^2]$ of water = 1 [mm] = 0.1 [cm].

      ii. For snow water equivalent, the original units are in millimeters. To convert to centimeters, multiply by 0.1:

         o SWE [cm] = SWE [mm] * 0.1 [cm/mm]

i) Subset the data that corresponds to the study area of the Sacramento / San Joaquin basin.

j) All of the ancillary data sets needed to derive groundwater estimates will have to be anomalies with the same baseline as the GRACE data. To do this, we compute the mean between Jan. 2004 and Dec. 2009 for all variables of interest. Then, subtract that baseline from all monthly observations.

For simplicity, we use the original 2004-2009 baseline and subtract it from the ancillary data, keeping in mind that the selection of another baseline will also work.

k) Create a set of anomalies maps for an example time period (we use Sep. 2015) for the variables of interest: Soil Moisture, Snow Water Equivalent, Reservoir storage and GRACE Equivalent Water Thickness anomalies (Figure 2E):
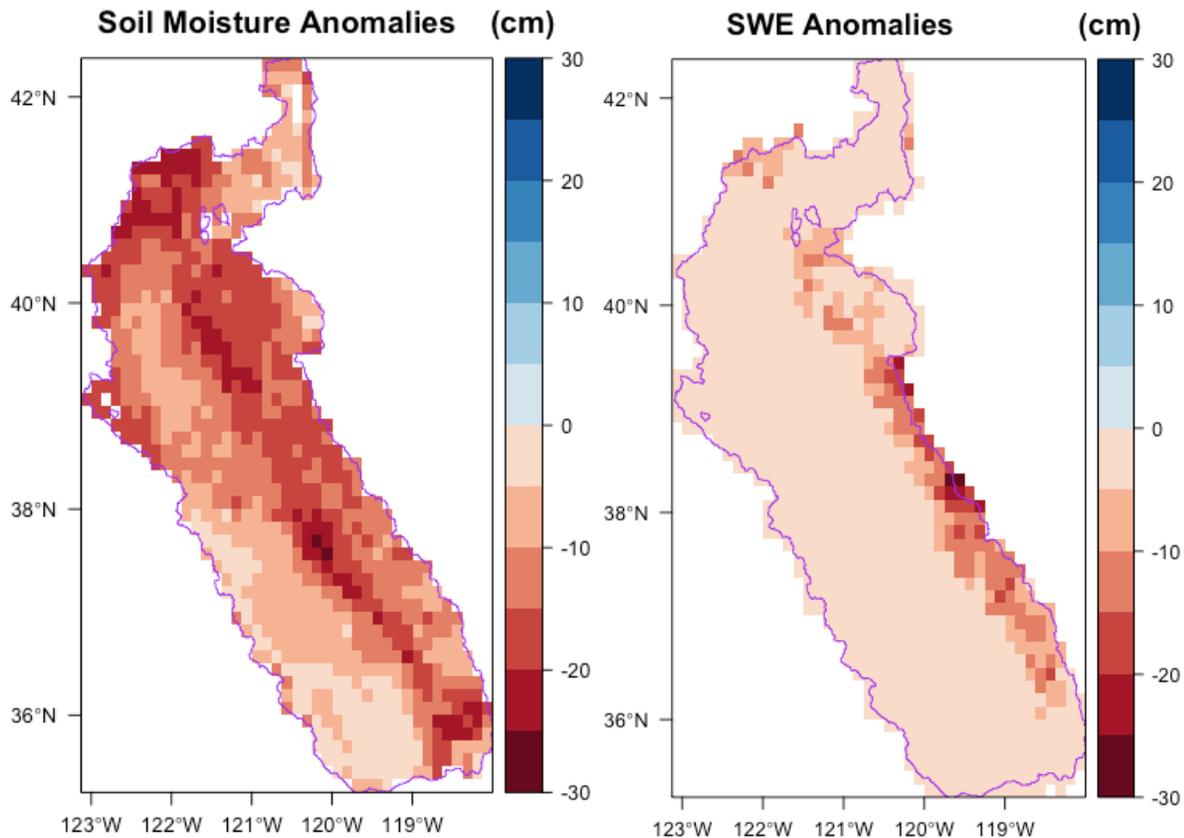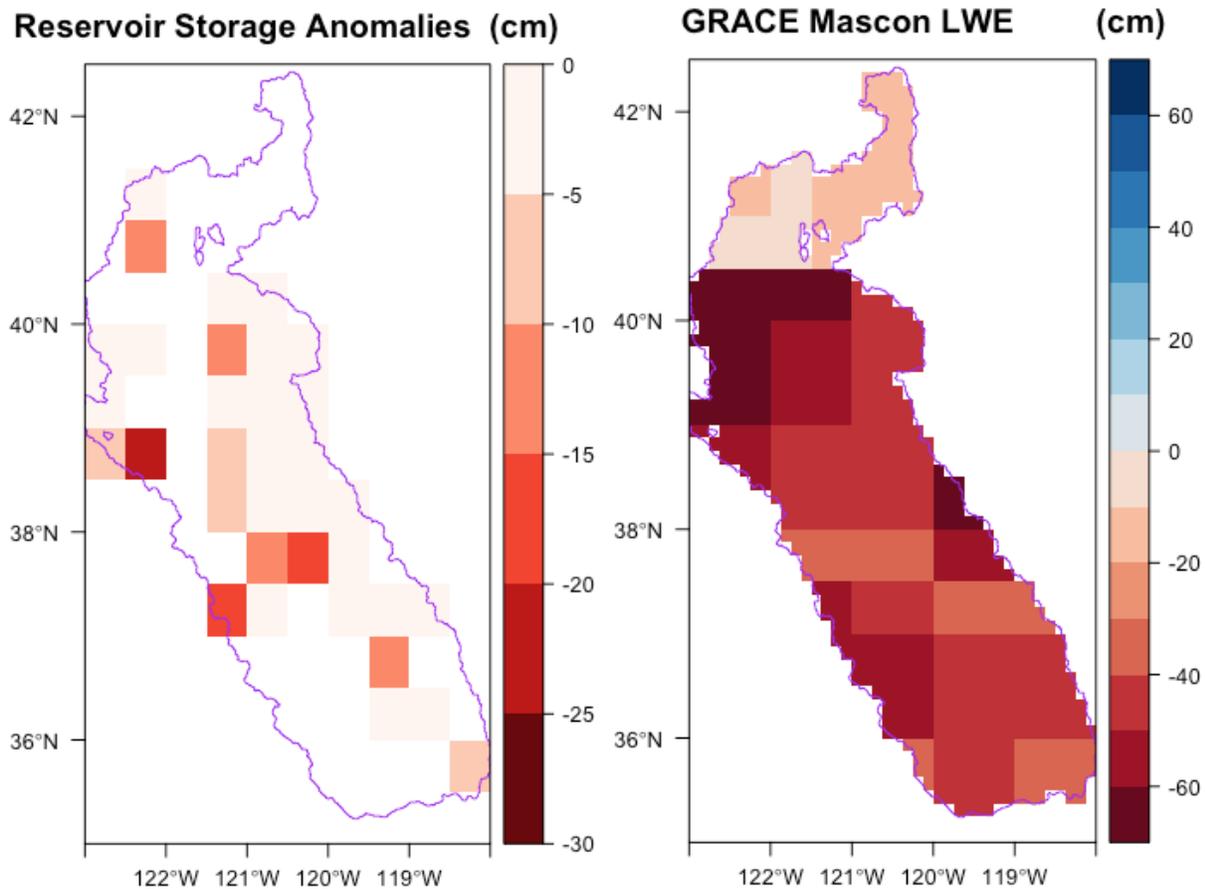
Figure 2E. Maps of the September 2015 anomalies for the variables of interest: Soil Moisture (top left), Snow Water Equivalent (top right), Reservoir storage (bottom left) and GRACE Equivalent Water Thickness anomalies (bottom right).

l) Aggregate the Soil Moisture and Snow Water Equivalent anomalies to match the more coarse 0.5 degree spatial resolution of the GRACE Mascon data.

m) Derive groundwater storage anomalies by subtracting Soil Moisture, Snow Water Equivalent, and reservoir storage anomalies from the GRACE Mascon Equivalent Water Thickness anomalies.

n) Create a time series of the input variables and of the final groundwater anomalies from 2004-2015 averaged over the Sacramento / San Joaquin basin (Figure 2F).

Mean Groundwater Anomalies
in the Sacramento / San Joaquin River Basin
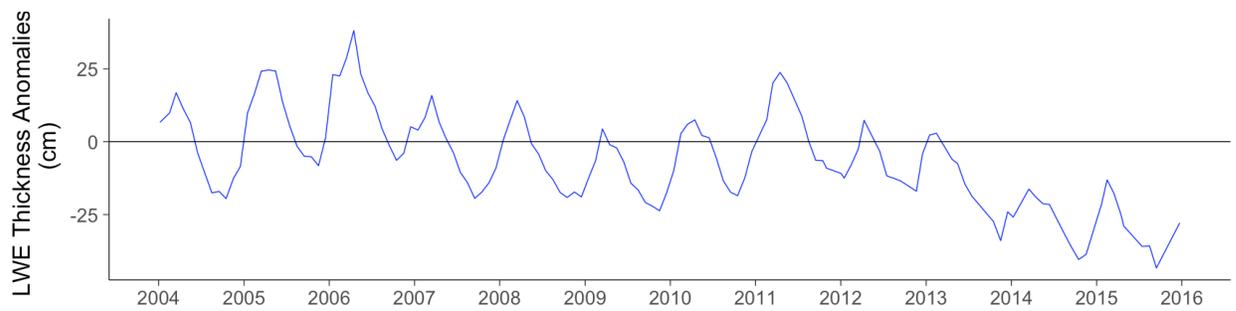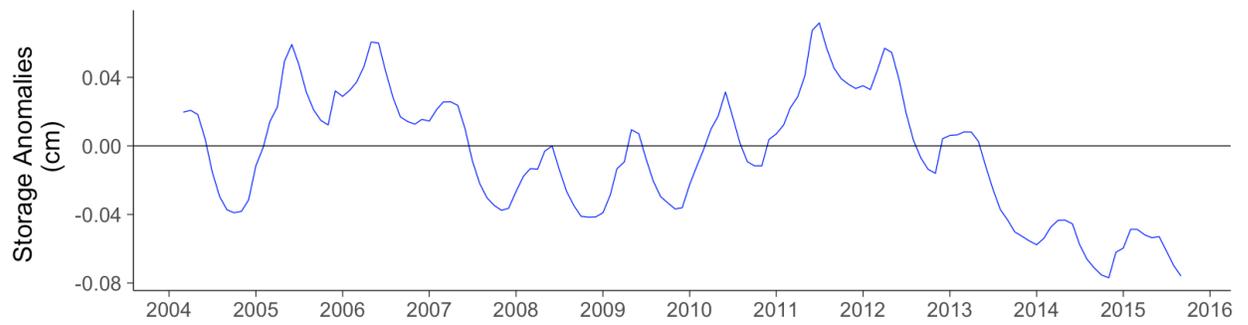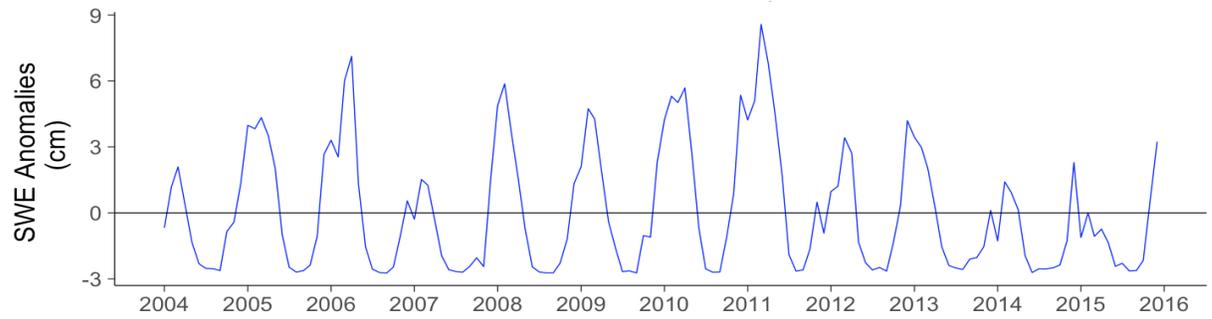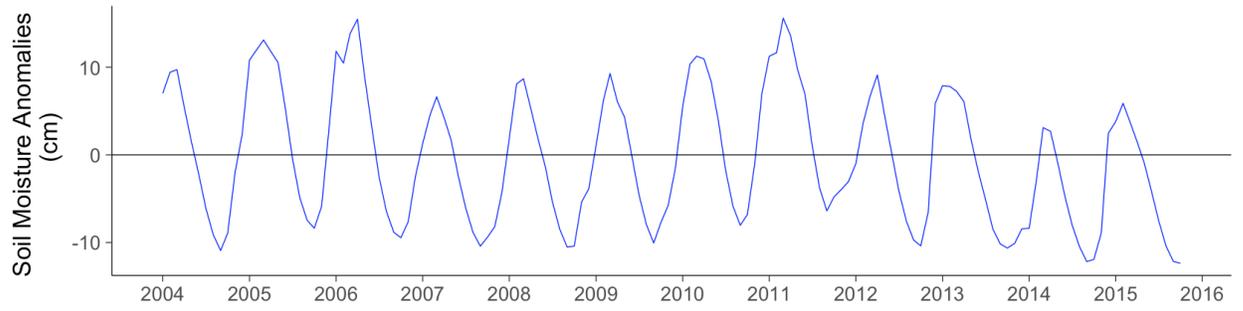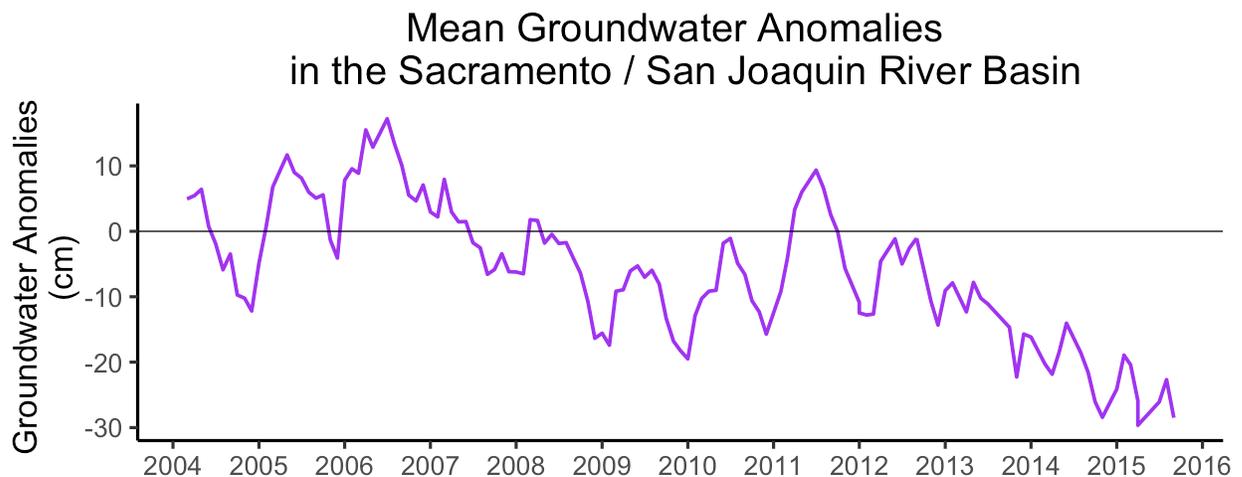
Figure 2F. Mean time series from 2004 to 2016 averaged over the Sacramento / San Joaquin basin for: Soil Moisture (top), Snow Water Equivalent (second from top), Reservoir storage (third from top), GRACE Equivalent Water Thickness anomalies (fourth from top), and ground water anomalies (bottom).

APPENDIX C: OCEAN MASS AND SEA LEVEL BUDGET

Step 1

a) Download the Level-3 gridded Mascon Terrestrial Water Storage anomalies data from GRACE Tellus website.

b) Download the land mask from GRACE Tellus website

c) Non-tidal variability is corrected for by using the time variable background model known as Atmosphere and Ocean De-aliasing Level-1B (AOD1B) (see section 3.3.6). The AOD1B product contains four different sets of Stokes coefficients characterizing the disturbing potential caused by anomalous masses in atmosphere and ocean. In this example, we will use 'GAD', which is the monthly average of 'oba' coefficients representing ocean bottom pressure simulated forced by atmospheric surface pressure and other meteorological quantities from the lower boundary of the atmosphere. In this application, only the global ocean mean of GAD is required, which is provided in TN12 at ftp://podaac.jpl.nasa.gov/allData/grace/docs/.

d) Download GIA-corrected Global Mean Sea Level (GMSL) time series data from sealevel.nasa.gov/ or directly access GMSL time series, called GMSL_TPJAOS_4.2_199209_201801.txt, here: ftp://podaac.jpl.nasa.gov/allData/merged_alt/L2/TP_J1_OSTM/global_mean_sea_level/).

   o Note that the Global Mean Sea Level (GMSL) data were produced by Brian Beckley from SGT, Inc. at NASA Goddard Space Flight Center and funded by NASA MEaSUREs. The GMSL was generated using the Integrated Multi-

Mission Ocean Altimeter Data for Climate Research
(http://podaac.jpl.nasa.gov/dataset/MERGED_TP_J1_OSTM_OST_ALL_V2)

o It combines Sea Surface Heights from TOPEX/Poseidon, Jason-1 and
OSTM/Jason-2 with all biases and corrections applied and placed onto a
georeferenced orbit. This creates a consistent data record throughout time,
regardless of the instrument used.

o If you use these data in a publication, please cite: B. D. Beckley, N. P.
Zelensky, S. A. Holmes, F. G. Lemoine, R. D. Ray, G. T. Mitchum, S. D.
Desai & S. T. Brown, Assessment of the Jason-2 Extension to the
TOPEX/Poseidon, Jason-1 Sea-Surface Height Time Series for Global Mean
Sea Level Monitoring, Marine Geodesy, Vol 33, Suppl 1, 2010.
DOI:10.1080/01490419.2010.491029.

Step 2

e) Apply Land mask to isolate the ocean in GRACE mascons.

f) Compute the global mean of each GRACE mascon observation and save the resulting
time series as a table.

g) Remove the effect of atmospheric pressure by subtracting the GAD background model
from the global mean GRACE mascons time series.

h) Obtain ocean mass anomalies by adjusting for the difference in ocean density versus
freshwater density:

o Fresh water density is about 997 kg/m³. Meanwhile, density of ocean water at
the sea surface is about 1027 kg/m³. There are two main factors that make
ocean water more or less dense than about 1027 kg/m³: the temperature of the
water and the salinity of the water. Ocean water gets more dense as
temperature goes down. Higher ocean salinity also makes the water more
dense.

o In order to keep this use case simple, we will derive an estimate of ocean mass
anomalies by multiplying the GAD-adjusted GRACE mass anomalies time
series by a single constant of 1.03.

i) Plot the ocean mass anomalies data over time (Figure 3A).
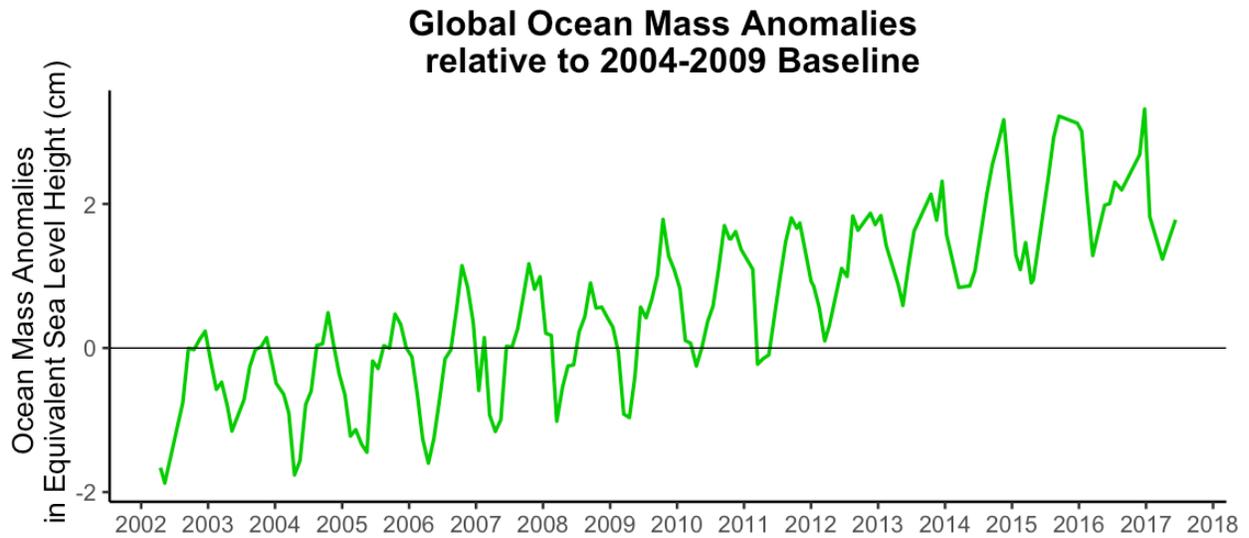
Figure 3A. Global ocean mass anomalies in equivalent sea level height from 2002 – 2016.

Step 3

   j)   Derive global sea level anomalies with a baseline to match the baseline of GRACE mascon data (Jan. 1, 2004 – Dec. 31, 2009)
- Subset the GIA-corrected global sea level altimetry data from Jan. 1, 2004 – Dec. 31, 2009.
- Compute the mean value of the 2004 – 2009 subset of data.
- Subtract the 2004 –2009 mean sea level value from each observation in the time series.
- Convert the units from mm to cm by multiplying each observation by 0.1.

   k)   Plot the sea level anomalies derived from the previous step (Figure 3B).
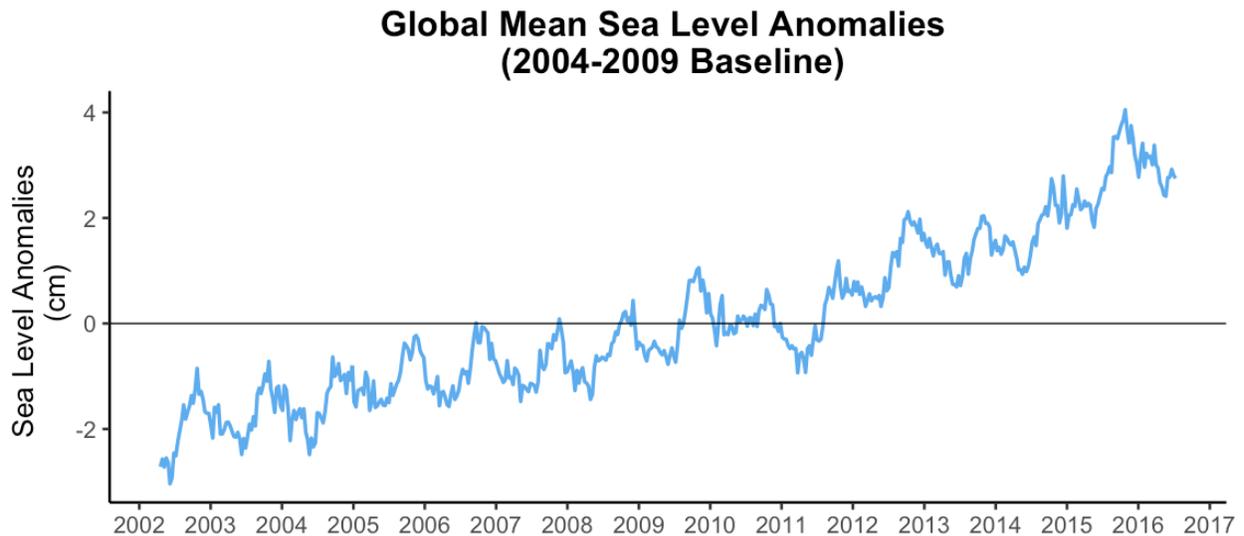
Figure 3B. Global mean sea level anomalies data from 2002 – 2016.

l) Derive the component of the sea level budget that can be attributed to thermal expansion by subtracting the ocean mass anomalies time series from the global mean sea level anomalies time series.

m) Produce a graph containing all three components: ocean height change attributed to thermal expansion, ocean mass anomalies and sea level anomalies from 2002-2016 (Figure 3C).
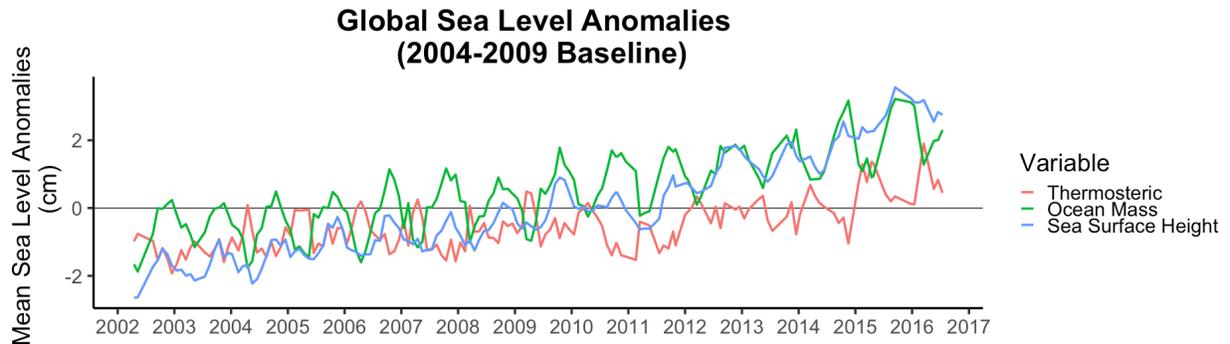

Figure 3C. Component of ocean height change attributed to thermal expansion (Thermosteric) plotted with ocean mass anomalies and sea level anomalies from 2002-2016

APPENDIX D: OCEAN CURRENTS & TRANSPORT

NOTE: This use case does not go as in-depth as the others. For more information on how to replicate the steps highlighted below, please refer to Landerer et a. (2015).

Background information:
The Atlantic Meridional Overturning Circulation (AMOC) consists of a northward flow in the upper layer of the ocean mostly between the surface and 1000 m depth and a return flow of North Atlantic Deep Water to the south in the deeper layers between 1000 and 5000 m. AMOC plays a key role in the poleward transport of heat. Changes in this transport can influence climate at higher latitudes significantly, with potentially significant impacts for the Northern Hemisphere (Intergovernmental Panel on Climate Change (IPCC), 2013).

Landerer et al. (2015) present the first measurements of Lower North Atlantic Deep Water transport changes using OBP estimates derived from GRACE. Large-scale AMOC flows are generally in geostrophic balance, and the meridional transport at a particular latitude and depth can be derived from the zonal Ocean Bottom Pressure (OBP) differences at the eastern and western basin boundaries of the Atlantic.

Summary of Steps:
3. Download the data:
   a. Level-3 gridded Mascon Terrestrial Water Storage anomalies data from GRACE Tellus website
   b. Ocean mask from GRACE Tellus website
4. Use GRACE ocean bottom pressure (OBP) mascons to characterize AMOC variations.
   c) Derive the meridional transport $T(y, z)$ at a particular latitude (y) and depth (z) by dividing the zonal bottom pressure differences $P_E(y, z)$ and $P_W(y, z)$ at the eastern and western basin boundaries by the Coriolis parameter (f) and the mean sea water density (ρ_0):

$$T(y, z) = \frac{P_E(y, z) - P_W(y, z)}{\rho_0 f}$$

   d) Integrating this between depth levels $z1$ and $z2$ yields the layer geostrophic AMOC volume transport from ocean bottom pressure data across the ocean basin:

$$T(y) = \frac{1}{\rho_0 f} \int_{z1}^{z2} P_E(y, z) - P_W(y, z) \, dz$$

The approach taken by Landerer et al. (2015) focuses on OBP anomalies in the layer of depth between 3000 m to 5000 m. The focus is on this layer because (1) it has a sufficiently large horizontal extent that can be resolved by GRACE, (2) it is relatively far away from land to avoid hydrological signal leakage, and (3) it corresponds to the so-called Lower North Atlantic Deep Water layer that is observed with the RAPID-MOCHA array. The step-like bathymetry from 3000 to 5000 m along the western boundary implies that the bottom pressure gradients here will

contribute most to the zonally averaged transport. More gently sloping topography would require additional information.

Concurrent with the observed AMOC transport anomalies from late 2009 through early 2010, GRACE measured OBP changes in the 3000–5000 m deep western North Atlantic on the order of 20 mm-H_2O (200 Pa), implying a southward volume transport anomaly in that layer of approximately −5.5 sverdrup (1 sverdrup = 1,000,000 m^3 s^{-1} = 264,000,000 USgal s^{-1}). Figure 4A shows OPB anomalies (mean of November 2009 through March 2010, relative to 2005–2012 mean) over the North Atlantic basin.
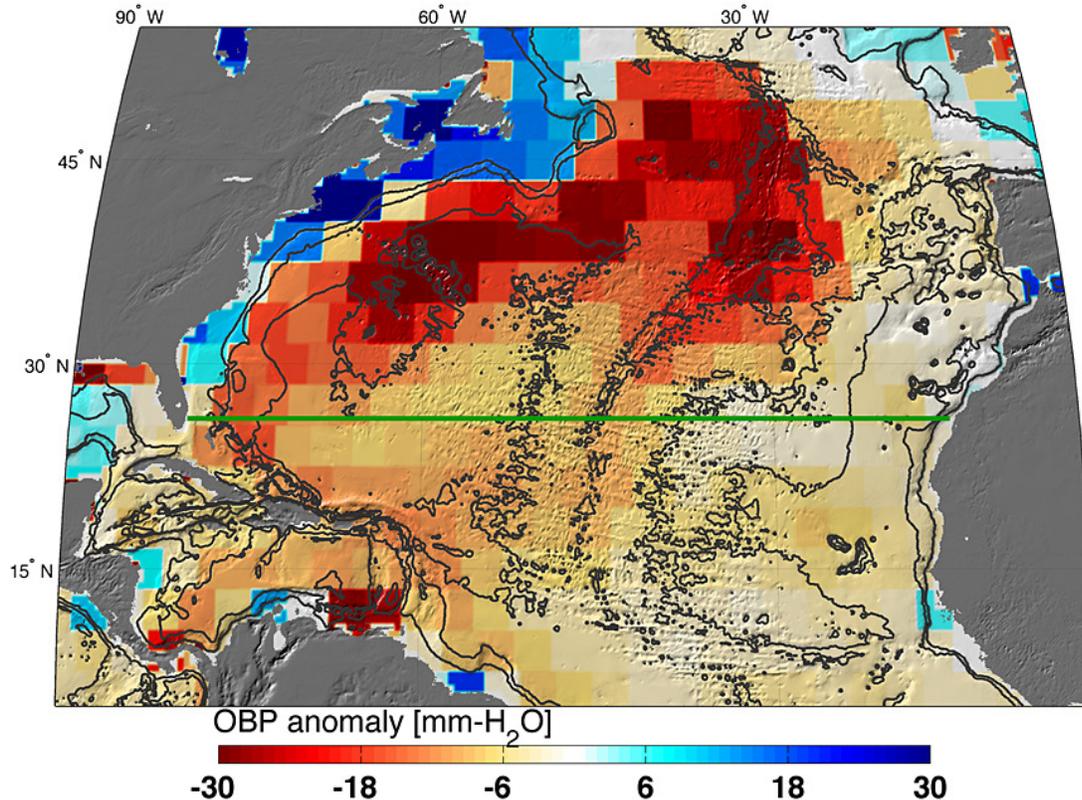

Figure 4A. Bottom pressure anomaly (mean of November 2009 through March 2010, relative to 2005–2012 mean) over the North Atlantic basin. Also shown is the location of the hydrographic in situ RAPID MOCHA section (green line; *Marotzke et al.*, 2002). Bottom pressure signals are largest on the western side of the basin and tend to be anticorrelated between shallow (0–1000 m) and deeper ocean regions (1000–5000 m) (see also Figure 1). One mm-H_2O OBP corresponds to approximately 10 Pa.

Results show that the detection of North Atlantic interannual OBP anomalies and Lower North Atlantic Deep Water transport estimates are in good agreement with those from the Rapid Climate Change-Meridional Overturning Circulation and Heatflux Array (RAPID/MOCHA) (Marotzke *et al., 2002;* Smeed *et al.*, 2014). The RMS difference between these two estimates is 1.2 sverdrup and the correlation is R = 0.69. The 1 sigma error of the GRACE-LNADW estimate is ±1.1 sverdrup (Figure 4B).
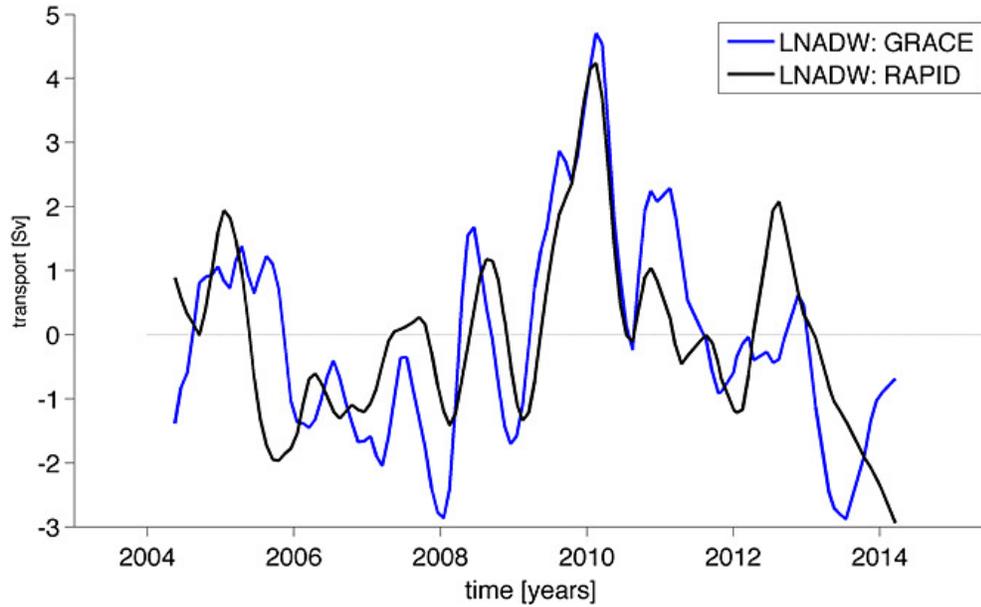
Figure 4B. Meridional transport estimates from GRACE OBP anomalies on the eastern and western margin integrated over the 3000–5000 m depth layer at 26.5N, compared to the RAPID-MOCHA estimate of LNADW. The RMS difference between these two estimates is 1.2 sverdrup and the correlation is R = 0.69. The 1 sigma error of the GRACE-LNADW estimate is ±1.1 sverdrup (from Landerer et al., 2015).